



# Process and material constraints of additive manufacturing for fabrication of terahertz quasi-optical components

Luke Phillips<sup>a,\*</sup>, Alexander Valavanis<sup>b</sup>, Andrew D. Burnett<sup>c</sup>, Robert Kay<sup>a</sup>,  
Russell Harris<sup>a</sup>, Ehab Saleh<sup>a,d</sup>

<sup>a</sup> School of Mechanical Engineering, The University of Leeds, Leeds LS2 9JT, UK

<sup>b</sup> School of Electronic and Electrical Engineering, The University of Leeds, Leeds LS2 9JT, UK

<sup>c</sup> School of Chemistry, The University of Leeds, Leeds LS2 9JT, UK

<sup>d</sup> College of Engineering and Technology, University of Doha for Science and Technology, Doha, Qatar

## ARTICLE INFO

### Keywords:

Quasi-optical components  
Additive manufacturing  
3D-printed THz optics  
Terahertz time-domain spectroscopy  
THz refractive index  
THz absorption coefficient

## ABSTRACT

Additive Manufacturing (AM) is an emerging fabrication method for terahertz-frequency (THz) quasi-optical components, allowing for the creation of complex geometries at an unprecedented short lead time whilst being a cost-effective production method. However, many 3D-printable materials have sub-optimal material properties at THz frequencies, while several AM processes lack the resolution required to produce optical components suitable for operation above 1 THz.

This work reviews the THz response of a range of AM materials, analysing their optical properties. Additionally, relevant AM process factors for manufacturing THz optics are evaluated, including the achievable minimum feature size, surface roughness and build rates, across AM process categories.

Studies demonstrate that AM processes capable of fabricating sub-100  $\mu\text{m}$  features, including vat photopolymerization, have the spatial resolution necessary for optics operating at frequencies above 1 THz. However, they have a limited material choice of absorptive photopolymer resins. In contrast, material extrusion enables access to a wider range of materials, including non-polar polymers that are highly transparent at THz frequencies. However, it offers poor resolution and produces rough surfaces relative to the wavelength of the THz region.

This review has identified several areas for future investigation, including the THz characterisation of AM-manufactured ceramics and composites, which could offer desirable properties for THz optics.

## 1. Introduction

The terahertz-frequency (THz) band of the electromagnetic spectrum includes frequencies ranging from approximately 0.1–10 THz and corresponding wavelengths ( $\lambda$ ) from around 3000–30  $\mu\text{m}$ , encompassing the millimetre and sub-millimetre bands [1]. Radiation in the THz region has a wide range of potential applications, including communication, spectroscopic and imaging applications. Due to their high frequency, THz waves can act as carriers for high-bandwidth wireless communications [2]. THz radiation also has the potential for material characterisation [3] and, being non-ionising, has desirable properties for both medical imaging and diagnostics [4].

However, the development of THz systems has, to date, been limited by a lack of manufacturing capability for quasi-optical components.

Typical infrared/visible optical materials are opaque at THz frequencies, and as such, the range of commercial off-the-shelf optical components is limited. Conversely, reflective quasi-optics and polymer-based lenses have an order-of-magnitude stricter dimensional tolerances in the THz band, compared with mm-wave, leading to higher scattering losses [5]. As such, new materials, and manufacturing techniques for optics in this range are highly desirable.

Additive Manufacturing (AM) offers a potential solution to these challenges and can produce complex, lightweight, and low-cost THz components. AM is already being used to produce THz quasi-optical components including, lenses, filters, waveguides, polarizers and phase plates [5–8]. AM technologies can produce complex geometric features including thin walls, hollow structures with internal cavities, lattice geometries and helical structures [9]. These complex features

\* Corresponding author.

E-mail address: [mnlcjp@leeds.ac.uk](mailto:mnlcjp@leeds.ac.uk) (L. Phillips).

<https://doi.org/10.1016/j.apmt.2025.102619>

Received 11 November 2024; Received in revised form 15 December 2024; Accepted 27 January 2025

Available online 1 February 2025

2352-9407/© 2025 The Author(s). Published by Elsevier Ltd. This is an open access article under the CC BY license (<http://creativecommons.org/licenses/by/4.0/>).

allow for greater flexibility to create a range of quasi-optical designs which would be challenging or impossible to produce using conventional manufacturing techniques. Examples include freeform lenses and waveguides with internal features [6,10]. This added manufacturing capability could drive further advancements in the development of quasi-optics.

However, several factors typically restrict 3D-printed components from operating at frequencies above 1 THz. One such aspect is that the most readily accessible AM processes do not have the necessary spatial resolution to produce microfeatures with smooth surfaces, required to reduce the attenuation of THz waves [11]. As the size of an optical component is typically proportional to the desired wavelength, THz optics require feature sizes on the  $\sim 10 \mu\text{m}$  scale, which push the limits of AM [12]. Lower-resolution AM processes also have high levels of surface roughness which increases scattering losses at THz frequencies [13].

Another limitation of using AM is a lack of available materials with suitable properties at THz frequencies. The optical properties of materials have often been compared in literature [14,15]. However, existing studies typically limit the comparisons to one AM process category or material type and can be limited in the frequency range they cover.

Therefore, the focus of this review will be to examine the potential of AM for the fabrication of THz quasi-optical components. Firstly, the characteristics of a range of AM materials will be discussed, with a focus on their refractive and absorptive properties at THz frequencies. Secondly, the process limits of AM technologies will be examined by investigating the minimum feature size, surface roughness and build rate. The review will culminate with a discussion indicating which AM technologies and materials are the most appropriate for the manufacture of exemplar optical components such as THz lenses. The review will aim to provide clarity on AM's potential in the field and provide focus to future research.

## 2. AM material types & properties at THz frequencies

Due to the design restrictions and costs of conventional and high-

resolution manufacturing techniques, research into using additive manufacturing (AM) to manufacture quasi-optical THz components is a rapidly expanding research area [11,16].

AM is a broad group of manufacturing processes with the general principle being that a 3D geometry is created by layering material. ISO/ASTM 52,900 defines seven AM process categories, with Material Extrusion (ME), Powder Bed Fusion (PBF) and Vat Photopolymerization (VP) being the most widely used [17]. Research has demonstrated that ME, VP, PBF and Material Jetting (MJ) are capable of fabricating THz waveguides, optics, substrates, and filters [5]. Examples of these components are shown in Fig. 1. The majority of these are passive dielectric devices for THz systems [7].

Quasi-optical devices are essential components for THz systems, being required to direct and shape THz radiation [21]. The material properties required for various quasi-optical devices are dependent on the wave-guiding mechanism. Mirrors are composed of highly reflective materials to ensure THz radiation is efficiently reflected. Whereas lenses often require low-loss materials that exhibit high levels of transparency, alongside a suitable refractive index for the chosen application.

Terahertz Time Domain Spectroscopy (THz-TDS) is commonly used to investigate the properties of materials at THz frequencies. This technique involves directing broadband THz pulses onto a material followed by ultrafast sampling of the transmitted THz field in the time-domain. The complex permittivity can then be determined from these measurements [22], in addition to the layer thickness of multi-layer samples [23]. Several studies have used this method to characterise the properties of AM materials at THz frequencies [14,24].

Existing research has focused on investigating the properties of 3D printed polymers at THz frequencies, largely because many non-polar materials are highly transparent to THz radiation and have the potential to be used for THz lenses and windows [24,25]. Non-polar polymers are used for THz applications due to their low absorption coefficients with high-density polyethylene (HDPE), polytetrafluoroethylene (PTFE) and polymethylpentene (PMP or TPX<sup>TM</sup>) being popular material choices for moulded components such as optics [26]. In contrast, polar polymers such as polyvinyl chloride (PVC), polyethylene terephthalate (PET) and

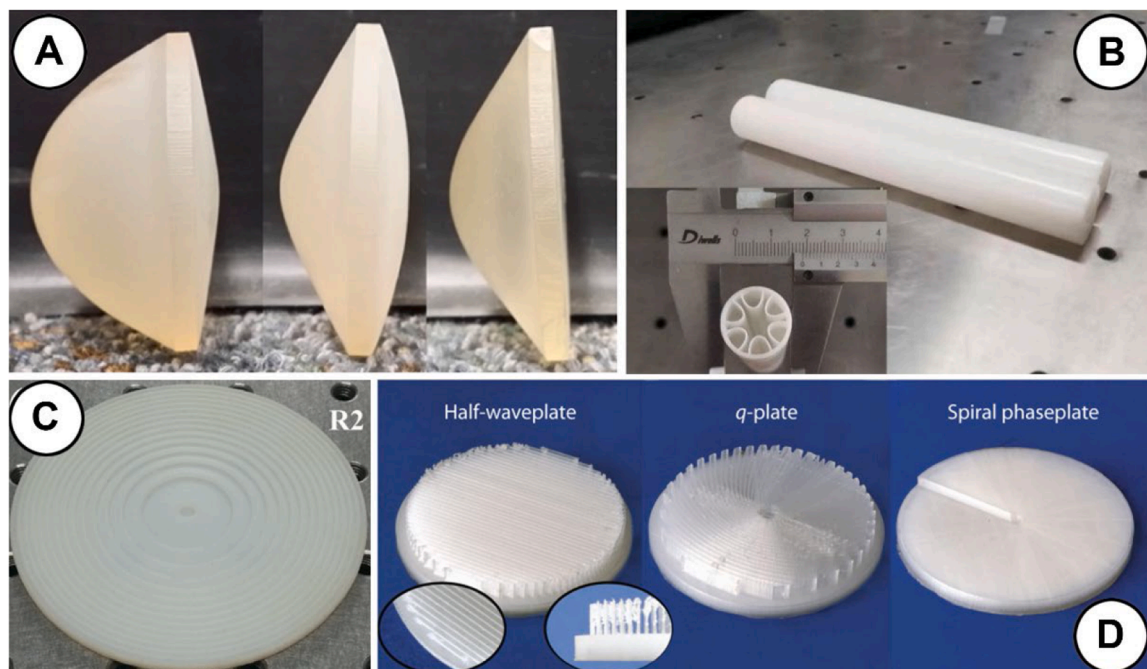


Fig. 1. (A). 3D printed THz domain aspherical lenses. Reproduced with permission [18]. Copyright 2015, Springer Nature. (B). SLA printed 15 cm long fibre. Reproduced under terms of the CC-BY licence [19]. Copyright 2021, Yang et al., Published by IEEE. (C). Polyjet printed THz phase plate. Reproduced under terms of the CC-BY licence [8]. Copyright 2017, Liu et al., Published by Scientific Reports. (D). FDM printed Cyclic Olefin Copolymer THz waveplates. Reproduced with permission [20]. Copyright 2021, Optica Publishing Group.

nylon have higher levels of THz absorption owing to larger dipole moments in the materials [27].

As THz radiation is unable to penetrate metals and highly polar materials, metals including gold, silver and aluminium are used for THz mirrors owing to their high reflectivity [28,29]. Studies have demonstrated that metal AM techniques including selective laser melting (SLM) can be used to manufacture reflective optics and devices designed to guide and focus THz radiation. However, SLM produced devices have significant losses owing to their high surface roughness compared to more traditional manufacturing techniques [30]. The refractive and absorptive properties of AM metal powders in the THz band are an under-researched area, likely owing to metal AM systems being a costly and less accessible AM technology [31].

The review will compare the properties of AM-printed polymers, photopolymers, and composites at THz frequencies, highlighting the properties achievable with different AM processes and the influence of parameter optimisation on material properties.

### 2.1. The refractive index of am materials at THz frequencies

The real refractive index ( $n$ ) is a key property for THz optics, determining the amount THz waves refract when transmitting through a material. Polymers with high transparency in the THz region typically have a low refractive index ( $n \approx 1.5$ ), as this minimises reflection loss from surfaces [32].

The refractive index often correlates with a materials density with more dense materials having a higher refractive index, for example,  $\text{Al}_2\text{O}_3$  with a density of  $3.99 \text{ g/cm}^3$  has a refractive index  $> 3$  at 1 THz [33]. However, the refractive index is also influenced by the materials structure and composition and the relationship between density and refractive index is not directly proportional for dense materials [34,35].

A moderate to high refractive index ( $n = >1.55$ ) is typically required to effectively direct and bend THz waves, a higher refractive index allows for thinner lenses to be produced with shorter focal lengths [36]. For thin lenses this is demonstrated by the lens maker's Eq. (1) with the focal distance of the lens ( $f$ ) being determined by both the refractive index ( $n$ ) of the material and the radius of the curvature of the first surface ( $R_1$ ) and second surface ( $R_2$ ) of the lens [37].

$$\frac{1}{f} = (n - 1) \left[ \frac{1}{R_1} - \frac{1}{R_2} \right] \quad (1)$$

A material with a higher refractive index allows for a reduced radius of curvature and thickness. However, a material with a higher refractive index suffers from larger reflection losses owing to the change in the refractive index of air and the material when interfacing. Anti-reflective coatings can be applied to materials with a high refractive index to reduce these losses.

Conventional polymer moulded THz lenses typically have refractive indices between  $n = 1.4 - 1.5$  [38] comparable to the refractive indices used for visible optics. Higher  $n$  values would allow thinner refractive lens geometries to be achieved, and hence a potential reduction in transmission loss. However, this is typically at the expense of higher surface Fresnel reflectance and greater chromatic aberration.

Polar polymers are typically dispersive in the THz region, meaning their refractive index varies with frequency [39]. However, non-polar polymers such as polystyrene (PS) show weaker dispersion, having a relatively constant refractive index, desirable for broadband optical components [25,27]. Additionally, studies have shown that the refractive index of polymers at THz frequencies is temperature-dependent, decreasing as temperature rises [40]. For example, a polypropylene (PP) sample was shown to have a refractive index of approximately 1.56 at 1.2 THz and 298 K, decreasing to around 1.55 at the same frequency when heated to 373 K [41].

Several studies have used THz-TDS to identify the refractive indices of a range of AM materials including polymer filaments [7,14],

photopolymers [15] and more recently ceramics [26] and composites [24]. However, the refractive index of the same material can vary for each THz-TDS measurement owing to differences in both the method of sample preparation and the measurement technique used to characterise the sample [42,43].

To investigate the refractive index of various AM materials data was gathered from studies investigating the optical properties of AM-produced samples. Fig. 2 showcases the collected result set for polymer filaments compatible with the ME process. As shown, the recorded refractive index of filaments has a large range from 1.48 to 1.79, with polyvinyl alcohol (PVA) having the highest value. These results compare with existing research showing that non-polar polymers typically have a refractive index lower than or around 1.55. Whereas polar polymers are in the region of 1.60 at 1 THz [27].

To compare different AM processes, the refractive index of photopolymers compatible with VP and MJ were also examined over the same frequency range (Fig. 3). All photopolymer samples were fabricated using AM systems, except for Phrozen Clear, which was cured in a mould under UV light. Most photopolymers are shown to have a similar refractive index between 1.61 and 1.72 with RC-90 having the highest recorded value at 1.72.

Fig. 4 shows the range of refractive indices categorised by the process. ME filaments have the widest range with recorded refractive indices between 1.48 and 1.79. VP has a smaller range than ME, ranging between 1.61 and 1.72 and MJ has the smallest range: between 1.66 and 1.69. MJ is generally a less accessible technology compared to ME and VP and has a limited number of compatible materials.

The larger refractive index range of filaments would allow for greater flexibility when designing THz optics, allowing for more compact and efficient components. However, a refractive index range of 1.48–1.79 is still relatively low, with higher refractive indices being desirable for certain THz optics to refract radiation at more extreme angles [45,50]. Therefore, research is ongoing to discover AM materials with higher refractive indices.

### 2.2. The absorption coefficient of AM materials at THz frequencies

The absorption coefficient ( $\alpha$ ) is another key property for THz optics, determining the amount of THz radiation absorbed per unit length as it passes through a material. It is typically measured in units of inverse length, (i.e.  $\text{cm}^{-1}$  or  $\text{m}^{-1}$ ).

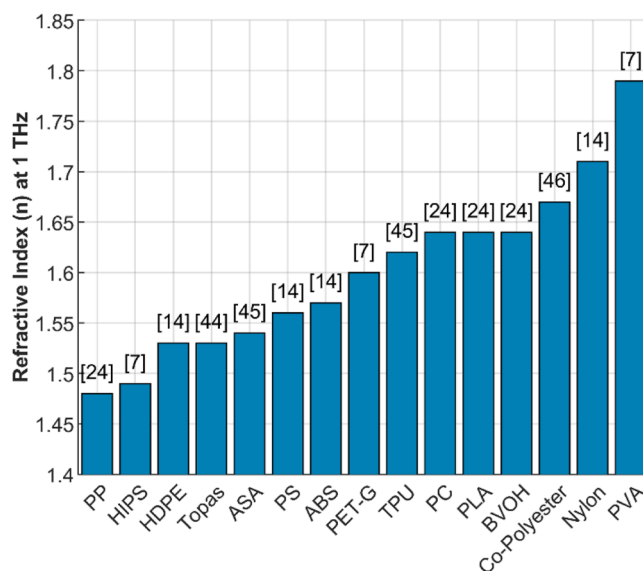


Fig. 2. The refractive index of 3D-printable materials compatible with ME at 1 THz, data obtained from references cited in [7,14,24,44–46].

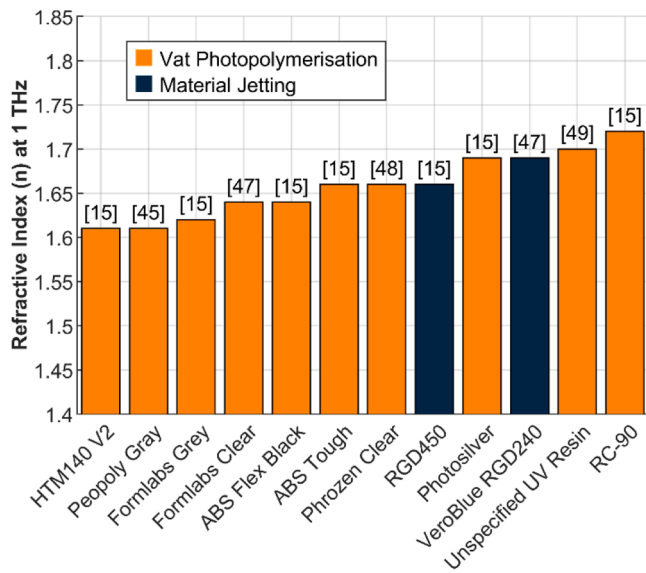


Fig. 3. The refractive index of 3D-printable photopolymers compatible with VP & MJ at 1 THz, data obtained from references cited in [15,45,47–49].

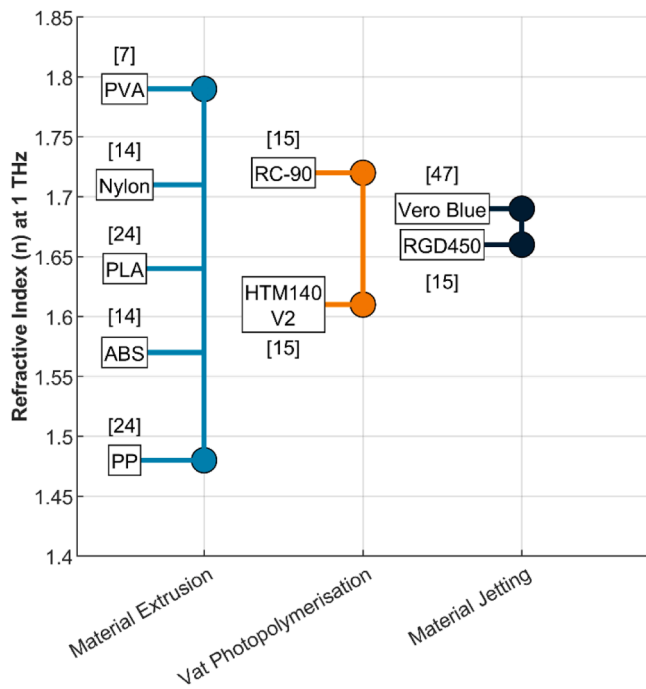


Fig. 4. The refractive index of AM materials at 1 THz, categorised by process, data obtained from references cited in [7,14,15,24,47].

A low absorption coefficient is essential for THz lenses, ensuring that there is minimal loss as the THz beam transmits through the optic. Therefore, materials are often chosen for these applications with low absorption coefficients at THz frequencies, typically below  $10 \text{ cm}^{-1}$  [45]. However, commercially available moulded lenses produced from TPX™, Cyclic Olefin Copolymer (COC) and PTFE have an absorption coefficient  $< 1 \text{ cm}^{-1}$  at 1 THz.

The absorption coefficient of polymers is determined by their molecular structure. Differences in crystallinity, branching and the number of polar bonds influence the types of vibrational modes and the energy required to excite them, affecting the amount of THz radiation absorbed [51]. Polar polymers, including PVC, polymethyl methacrylate (PMMA) and PET exhibit higher absorption of THz due to them having an uneven

charge distribution and large changes in dipole moments during the molecular vibrations that correspond to the THz region [39,52]. Although non-polar polymers still have vibrational modes at THz frequencies, the changes in dipole moment during these vibrations are generally much weaker, resulting in fewer absorption peaks in their spectra and a lower absorption coefficient than polar polymers [39].

Over the past decade research has been ongoing to record the absorption coefficient of several AM materials using THz-TDS [14,24]. However, just like the refractive index the absorption coefficient of the same material can vary depending on sample preparation, or measurement technique.

To examine the absorption coefficient of AM materials at 1 THz, data was collected from a range of studies. Fig. 5 highlights the absorption coefficients of AM-produced samples produced from various filaments at 1 THz. As shown, the absorption coefficients of these polymers range significantly with more established AM materials, including polylactic acid (PLA), PVA and Nylon being presented as highly absorptive materials with absorption coefficients ranging from  $27 - 32 \text{ cm}^{-1}$ . These results also compare with existing research comparing polar and non-polar polymers at THz frequencies, with polar polymers having a higher absorption coefficient [39].

Less commonly used filaments are shown to be highly transparent with HDPE, Topas/COC and PS having recorded absorption coefficients under  $3 \text{ cm}^{-1}$  at 1 THz. Although these materials are less absorptive to THz radiation they can be challenging to print for example, HDPE is significantly more difficult to manufacture using Fused Filament Fabrication (FFF) owing to its high-temperature expansion coefficient [14].

Fig. 6 presents the absorption coefficient values of 3D printed samples made from a variety of photopolymers, except for Phrozen Clear, which was UV-cured in a mould. As shown photopolymers have a high absorption coefficient at 1 THz between  $19 - 27 \text{ cm}^{-1}$ . Studies have also demonstrated that the absorption coefficient of photopolymers beyond 1 THz rapidly increases [15], limiting their potential to be used for quasi-optical components at frequencies higher than 0.3 THz [47].

The properties of polymer powders compatible with PBF were also searched for however, no relevant data could be found. This is likely due to the powders typically used in PBF having high absorption coefficients. For example, Selective Laser Sintering (SLS) typically prints using nylon powder [54]. As previously highlighted nylon is an absorptive material at THz frequencies and is unsuited for optical devices which could

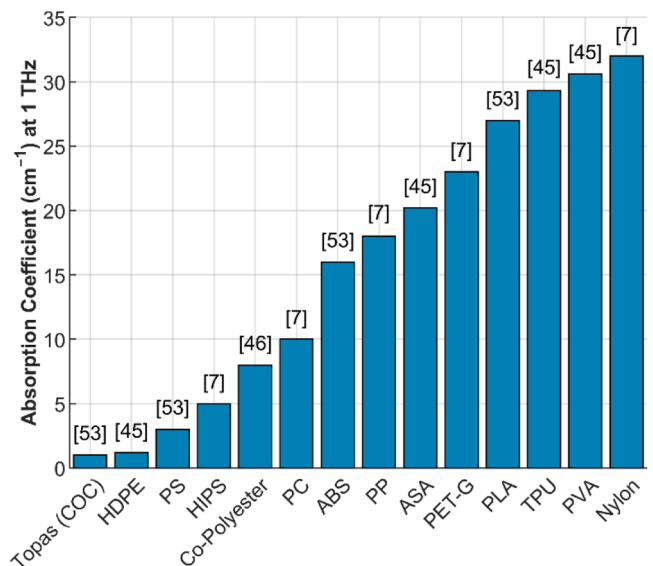


Fig. 5. The absorption coefficient of 3D printable materials compatible with ME at 1 THz, data obtained from references cited in [7,45,46,53].

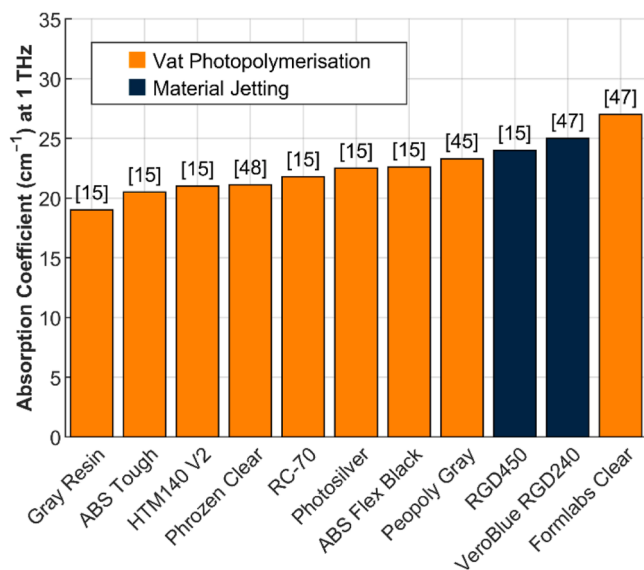


Fig. 6. The absorption coefficient of photopolymers compatible with VP & MJ at 1 THz, data obtained from references cited in [15,45,47,48].

explain the lack of research.

Fig. 7 shows a comparison of the recorded absorption coefficient values of AM materials categorised by the process. As shown ME offers the greatest range of properties being suitable for absorptive components including filters and low-loss elements such as lenses.

Photopolymers produced using MJ and VP are shown to be generally absorptive and would not be suitable for low-loss THz applications. However, the composition of photopolymer resins can vary significantly, with the choice of monomer and photoinitiator significantly altering the polymer's composition. Most AM photopolymer resins are acrylic/methacrylate-based, as this composition allows for fast printing speeds owing to its free radical polymerization mechanism [55]. However, vinyl ether and epoxy resins are also available but less commonly used [56].

As many commercially available resins are acrylic-based, including

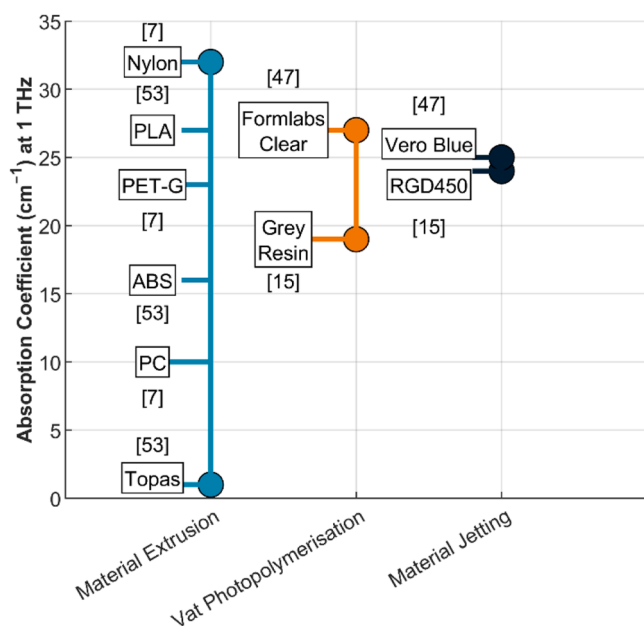


Fig. 7. The absorption coefficient of AM materials at 1 THz categorised by process, data obtained from references cited in [7,15,47,53].

many of the Vero and Formlabs material family [57,58], studies have primarily focused on these. The characterisation of a broader range of photopolymer resin formulations with varying compositions of monomers and photoinitiators could identify resins with an increased range of spectral properties.

### 2.3. The influence of AM process parameters on THz properties

Although it is useful to compare the properties of AM materials at THz frequencies, the properties of a material can be influenced by the printing parameters chosen. For FFF parameters including the nozzle diameter, printing pattern and layer thickness are shown to affect the refractive index and absorption coefficient of AM samples [59]. This is largely owing to these parameters affecting the porosity of the printed material [60]. Research shows that adjustment of the layer height and print direction can reduce the porosity of FFF-printed components from around 7 % to 2 % [61].

Higher amounts of porosity in 3D printed components can increase the amount of scattering loss owing to the interaction of the THz waves with air voids within the material. However, increased porosity can also reduce absorption as it reduces the density of the printed material, with air having a lower absorption coefficient and refractive index. To reduce the porosity of FFF-printed components caused by print defects, machine learning and process monitoring systems could be integrated. Studies have demonstrated that voids and defects within printed components can be detected using *in situ* thermal and optical cameras [62, 63]. Therefore, process monitoring systems could help to certify FFF-printed quasi-optical components, reducing variability between batches.

Fig. 8(A) demonstrates how optimising the parameters of FFF systems altered the optical properties of printed COC samples. Reducing the nozzle size from 600 to 150 μm and changing the printing temperatures

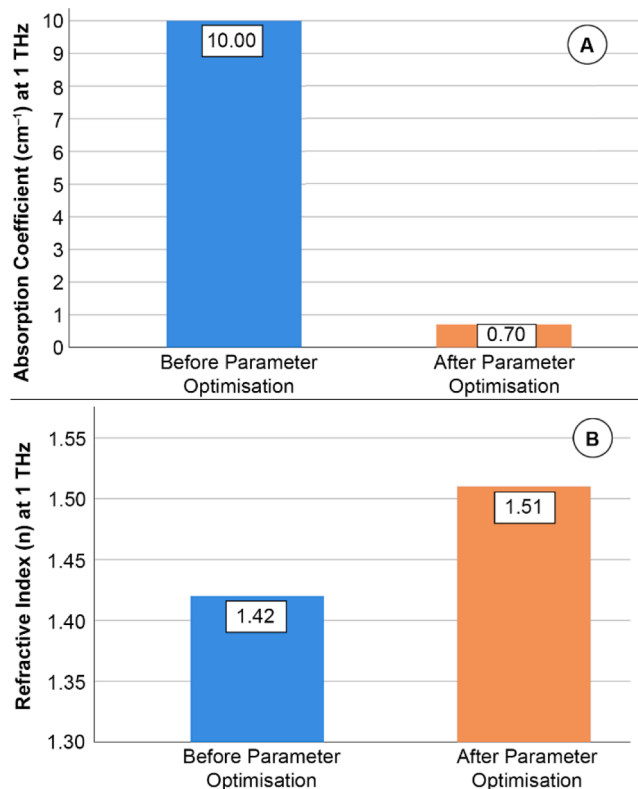


Fig. 8. (A). The absorption coefficient of FFF printed COC samples at 1 THz before & after parameter optimization, data obtained from [44]. (B). The refractive index of FFF printed COC samples at 1 THz before & after parameter optimization, data obtained from [44].

between a range of 190–260 °C reduced the absorption coefficient from 10 cm<sup>-1</sup> to around 0.7 cm<sup>-1</sup> at 1 THz. Fig. 8(B) shows that the changes also increased the refractive index of the sample from 1.42 to 1.51 [44]. These results show how changes to FFF printing parameters can alter the THz properties of AM materials, with optimised parameters allowing for the fabrication of 3D printed THz lenses with increased transparency and a higher refractive index.

Existing research has primarily investigated the influence of FFF build parameters and the resulting change in spectral properties at THz frequencies. However, a recent study fabricated photopolymer samples via Stereolithography (SLA) with ranging UV exposure settings. The results showed that the refractive index of the printed samples at 1 THz increased from approximately 1.71 with 1 mJ/cm<sup>2</sup> exposure to 1.76 with 10 mJ/cm<sup>2</sup> of exposure [64]. This work demonstrates that the build parameters for both VP and MJ, particularly the exposure level, can influence the optical properties of printed components at THz frequencies. However, the influence of various build parameters on VP, MJ and PBF systems is largely unknown.

### 2.4. THz optical properties of AM composites

Another consideration is that the spectral properties of materials at THz frequencies can be modified with filler materials, allowing the rational design of bespoke composites with desirable optical properties.

Fig. 9 showcases existing work characterising the properties of polymer composites at 1 THz. This research demonstrates that increased weight ratios of filler materials can influence both the refractive index and absorption coefficient of materials. As shown, the addition of quartz, a low-loss material, significantly decreased the absorption coefficient of a resin, whilst the addition of Titanium dioxide, a highly absorptive material, increased the absorption of the polyethylene (PE) composite. However, the examples in this figure were not processed using AM systems, polymers were compressed, moulded, or doped with filler materials to form composite samples suitable for THz characterisation.

Recent studies have recognised the potential of AM composite materials for THz applications, with recent work using THz-TDS systems to characterise materials which could be compatible with ME systems, including PLA composites [24], PP composites [29] and acrylonitrile

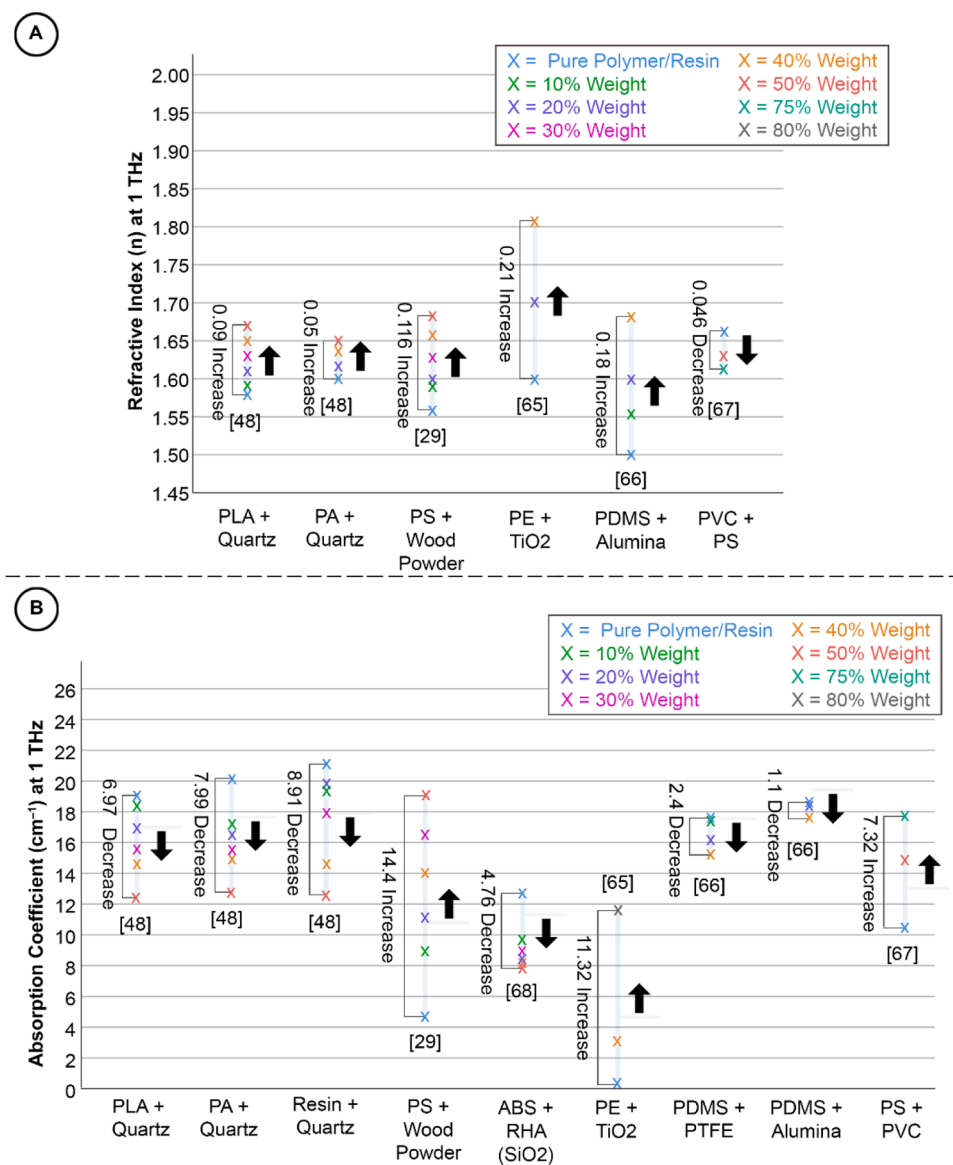


Fig. 9. Spectral properties of polymer composite materials produced via moulding, compression or doping, with varying weight ratios of filler materials (A) Refractive index of polymer composites at 1 THz, data obtained from references cited in [29,48,65–67]. (B) The absorption coefficient of polymer composites at 1 THz, data obtained from references cited in [29,48,65–68].

butadiene styrene (ABS) composites [68].

Fig. 10 shows the recorded refractive index of polymer composites compared to the base polymer. It shows the refractive index of PLA embedded with metal flakes increased from 1.64 to 2.10, with the composite material having a significantly higher refractive index.

Research characterising the absorption of polymer composites at THz frequencies also found that the absorption coefficient could increase or decrease depending on the properties of the filler material. As shown in Fig. 11, the addition of a highly absorptive metal, for example, Copper to PLA increased the absorption coefficient from 27 to 38.4  $\text{cm}^{-1}$ . Whereas, adding materials with lower absorption coefficients can decrease it, with an ABS composite consisting of 40 % Rice Husk Ash having a coefficient of 8.14  $\text{cm}^{-1}$ , significantly lower than ABS (16  $\text{cm}^{-1}$ ).

Although VP offers higher resolution than ME, only a handful of studies have investigated the properties of photopolymer composites [69]. A 2023 study characterised the properties of GP-silica, a photopolymer embedded with silica nanoparticles. It found that a 3D printed sample had an absorption coefficient of around 1.1  $\text{cm}^{-1}$ , far lower than any recorded photopolymer [70]. Previous research has also shown that the addition of high purity alumina samples to a photopolymer increased the index of refraction to around 3.09 at 1 THz [26]. However, both studies post-processed the materials, firing the samples to debind the photopolymer and sinter the ceramic particles and did not examine the properties of the printed (green state) composite.

There are also several challenges associated with printing photopolymer composites containing ceramic fillers using stereolithography, with extensive post-processing often being required to produce components with smooth surfaces [71], which is crucial for THz optical components. The addition of ceramic particles to photopolymer resins can also increase the viscosity of resins and reduce the penetration depth of UV light due to scattering effects, reducing the geometric accuracy of the printed component [72].

Overall, these studies demonstrate that the addition of a filler material can alter the absorption coefficient and refractive index of the resulting composite. Adding highly transparent filler materials with a high refractive index at THz frequencies to AM feedstock materials could enable the production of more efficient THz optics to be fabricated using 3D printing. However, further investigation of the properties of AM composites is required with current research being limited.

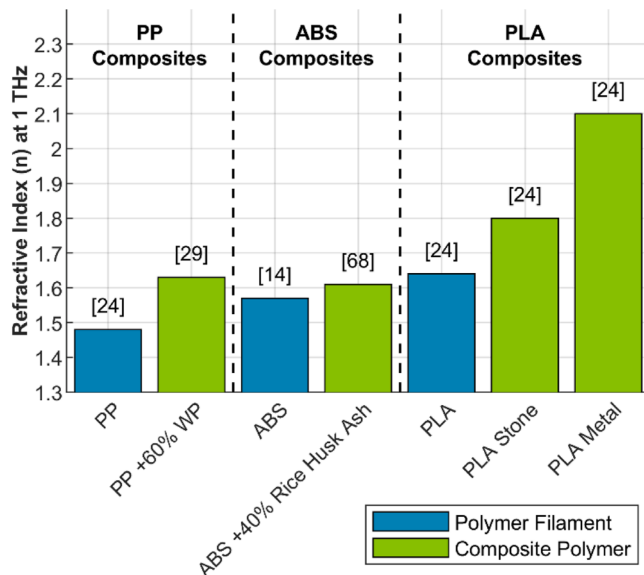


Fig. 10. The refractive index of polymers and polymer composites at 1THz, data obtained from references cited in [14,24,29,68].

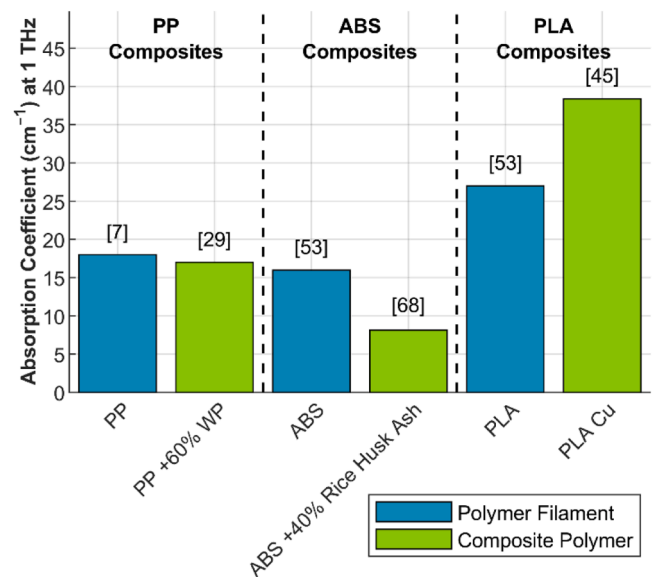


Fig. 11. The absorption coefficient of polymers and polymer composites at 1 THz, data obtained from references cited in [7,29,45,53,68].

### 3. The process characteristics of AM for quasi-optics production

#### 3.1. The minimum feature size of AM processes

As a THz device size is proportional to the desired wavelength [73]. This can rule out several AM technologies from producing quasi-optical components operational at frequencies above 1 THz, with AM-produced devices often being restricted to operating at frequencies between 0.1–1 THz [11].

This is owing to the wavelength of 0.1–1 THz corresponding to 3 mm - 300  $\mu\text{m}$ , with quasi-optical components requiring feature sizes an order of magnitude smaller than the wavelength, to ensure features on optical components do not scatter or distort THz waves [5,74]. As most AM processes can create minimum feature sizes below 100  $\mu\text{m}$  the technology is well suited to this frequency range [20].

At the higher end up to 10 THz the wavelength can range as low as 30  $\mu\text{m}$  [75]. At these higher sub-mm frequencies, the required minimum feature sizes can be in the region of or below 10–20  $\mu\text{m}$  [12]. These smaller feature sizes not being achievable with all AM processes.

Therefore, it is important to consider the process limits of different AM technologies to assess their suitability to produce THz devices. The recorded printable minimum feature sizes of six AM technologies were collected from multiple studies. This data was plotted to show the range of printable minimum feature sizes for each technology see Fig. 12.

As shown, many of these processes have the necessary resolution to create devices operational at sub-mm frequencies. VP has been shown to produce minimum feature sizes between 15 and 154  $\mu\text{m}$ . This positions it well for THz applications to be able to produce features at scales equal to or below THz wavelengths. MJ and PBF had similar levels of resolution being able to achieve minimum feature sizes under 50  $\mu\text{m}$ . ME produced the largest feature sizes with the smallest recorded feature being 200  $\mu\text{m}$ . This would be suitable for devices operational around 1 THz. However, lenses produced using ME with key features aimed at shorter wavelengths (>1 THz) may attenuate and distort THz waves, reducing the effectiveness of the 3D-printed optical component.

#### 3.2. The surface roughness of additive manufacturing processes

The surface roughness of AM-produced THz optics is a key consideration when selecting an AM technology, as the roughness value can directly influence the performance of the optical device.

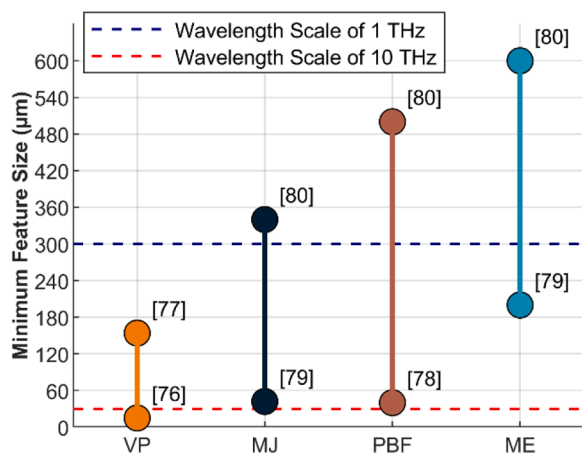


Fig. 12. Range of recorded feature sizes of AM processes, data obtained from references cited in [76–80].

Studies have demonstrated that a surface roughness value considerably below the operational frequency of optical components is required to ensure optimal transmission of THz. A recent study examined the transmission of PTFE samples sanded with 40, 60, 80 and 220 grit sandpaper, resulting in surfaces with Root Mean Square (RMS) roughness values of 222 µm, 164.5 µm, 105.5 µm and 56.6 µm respectively. At 1 THz ( $\lambda = 300 \mu\text{m}$ ), the PTFE sample with an RMS roughness of 105.5 µm exhibited a significant decrease in transmission, despite the roughness being approximately one-third of the wavelength. In contrast, the PTFE sample with an RMS roughness of 56.6 µm showed a minimal drop in transmission. Highlighting the requirement for THz optical surfaces to have a surface roughness considerably below the target wavelength [81].

High surface roughness in THz optics or substrates can result in diffuse scattering, as the interaction of the THz wave with a rough surface causes the wave to scatter, resulting in a loss of transmission. This attenuation reduces the performance of optical components. Therefore, manufacturing processes need to be selected based on their ability to produce smooth surfaces with roughness values considerably below the target wavelength.

The Rayleigh Criterion (2) helps to determine whether a surface is considered rough relative to the target wavelength of the incident radiation. The Rayleigh Criterion considers a surface as rough if the maximum height difference of the surface  $h_0$ , exceeds the critical height  $hc$ , which is determined by the wavelength  $\lambda$  of the incident beam and the angle of incidence  $\theta$ . The critical height is given by:

$$hc = \frac{\lambda}{8\cos\theta i} \tag{2}$$

If the maximum height difference of the surface  $h_0$ , exceeds  $hc$ , the surface is considered rough, with surface irregularities being large enough to scatter incident radiation affecting the performance of optical components [82].

A surface roughness of  $< \lambda/10$  is typically acceptable for optical components [83]. However, high-quality optical components and substrates aim for a surface roughness equivalent to  $\lambda/20$ , to minimize scattering and ensure enhanced performance [84]. The corresponding wavelength and indicative surface roughness benchmarks of  $\lambda/10$  and  $\lambda/20$  in the THz region (1–10 THz) are presented in Table 1. As shown the surface roughness benchmark of  $\lambda/20$  ranges from approximately 15 µm at 1 THz to 1.5 µm at 10 THz, reflecting the shortening of the wavelength with increasing frequency.

As previously highlighted AM technologies vary significantly in print resolution, influencing the level of surface roughness of printed components. A recent 2023 review by Golhin et al. examined the surface roughness of 3D-printed polymers, comparing the roughness values of

Table 1  
Guideline surface roughness benchmarks for 1–10 THz.

Frequency \ THz	Wavelength ( $\lambda$ ) \ $\mu\text{m}$	Surface Roughness ( $\lambda/10$ ) \ $\mu\text{m}$	Surface Roughness ( $\lambda/20$ ) \ $\mu\text{m}$
1 THz	$\approx 300$	30	15
2 THz	$\approx 150$	15	7.5
3 THz	$\approx 100$	10	5
4 THz	$\approx 75$	7.5	3.75
5 THz	$\approx 60$	6	3
6 THz	$\approx 50$	5	2.5
7 THz	$\approx 43$	4.3	2.15
8 THz	$\approx 37$	3.7	1.85
9 THz	$\approx 33$	3.3	1.65
10 THz	$\approx 30$	3	1.5

printed surfaces when printed using different AM process categories [85].

To assess whether AM processes are capable of manufacturing surfaces with roughness values comparable to the indicative benchmarks ( $\lambda/10$ ,  $\lambda/20$ ), the average roughness values (Ra) of surfaces produced using VP, MJ, PBF and ME were plotted using data obtained from the recent review by Golhin et al., see Fig. 13. Due to the high variation in surface roughness between side and top surfaces produced using ME both were plotted.

As shown both VP and MJ can manufacture smooth surfaces with Ra values  $< 15 \mu\text{m}$ , with VP achieving Ra values ranging from 0.025–2.86, meeting the requirements for high quality optics ( $\lambda/20$ ) in the THz region (1–10 THz).

ME and PBF were shown to produce surfaces with roughness values comparable to or below ( $\lambda/20$ ) at 1 THz. However, at frequencies above 3 THz, optical components produced using these processes would likely suffer from some level of attenuation owing to their higher surface roughness.

Both ME and PBF produce rougher surfaces than VP and MJ because they use thicker layer heights. The use of thicker printing layers and the layer-by-layer printing approach leads to a staircase effect, where new layers are deposited onto existing layers with differences in alignment producing visible ridges and steps [88,92]. The staircase effect is less pronounced with MJ and VP as they use thinner layer heights, resulting in smoother surfaces [93,94]. Side and top surfaces produced using ME have a high degree of variation in surface roughness, with side surfaces being typically rougher owing to the staircase effect, top surfaces are generally smoother as they are printed in a single path with the paths overlapping to reduce roughness.

Studies have demonstrated that the surface roughness of components

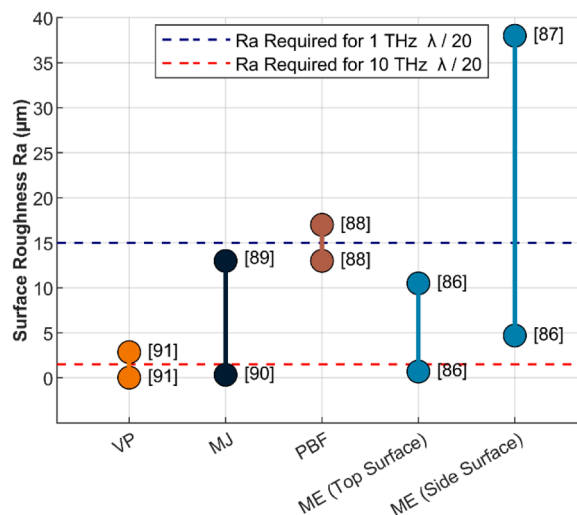


Fig. 13. Surface Roughness (Ra) of various AM process categories [86–91].

fabricated using ME and PBF is influenced by the chosen process parameters. For ME the most influential parameters are the layer height, infill density, part orientation, print speed and print temperature [95, 96]. The laser scan strategy is shown to impact the surface roughness of SLS-produced components as it influences the melting behaviour of powders and can lead to partially sintered powders adhering to sintered geometry, increasing surface roughness.

However, there are a range of post-processing options for 3D-printed components that can significantly improve the surface roughness of AM-produced surfaces. 3D-printed polymers are typically post-processed using mechanical abrasion (sanding or bead blasting), chemical treatments, or applied with a coating to smooth surfaces [97,98].

Although ME and PBF have been shown to produce rougher surfaces than MJ and VP, it has been demonstrated that the surface roughness of both can be improved through various post-processing methods. For ME, studies have shown that vapour smoothing can significantly improve the surface finish, reducing the Ra of a printed ABS surface from around 9.5 to 4.5  $\mu\text{m}$  [99]. Turek also found that both mechanical and chemical surface treatment could reduce the Ra of PBF-produced surfaces. Glass bead blasting was shown to reduce the Ra value of a printed PA12 sample to a Ra range of 9.5–13.3  $\mu\text{m}$ . Vapour smoothing further reduced this to a Ra range of 2–3.4  $\mu\text{m}$  [100]. Although post-processing can reduce surface roughness, it can be labour intensive and increase the overall cost of the 3D printed component. The dimensional accuracy of components can also be reduced, which is critical for quasi-optical components [101].

As demonstrated ME, PBF, VP and MJ can produce surfaces with roughness values comparable to or below the wavelength scale of the THz region (1–10 THz). Both VP and MJ are shown to be viable processes to produce THz optics, capable of fabricating smooth surfaces with roughness values comparable to  $(\lambda/20)$  at 10 THz, meeting the indicative benchmark for high quality optics without the need for post-processing. Studies have shown that surfaces produced using PBF and ME have higher levels of surface roughness. However, these processes may be suitable for producing optical components operating around 1 THz owing to the longer wavelength, or could be post-processed to achieve smoother surfaces, to reduce potential THz loss.

### 3.3. The build rate of AM processes

The build rate is a key consideration when choosing an AM process to manufacture THz components. Although the resolution of processes is key to a device's achievable operational frequency for many applications, it needs to be balanced against the processing rate of the technology. As THz applications grow the number of components required will increase substantially, for AM to be able to fulfil these manufacturing demands suitable processes will need to be chosen with high build rates for AM to be commercially viable.

To analyse this the build rates of several AM processes were collected. This data was then plotted to show the range of recorded build rates for five AM technologies see Fig. 14.

VP and PBF are shown to have relatively slow production rates in the region of 10 s of  $\text{cm}^3/\text{h}$ . ME can achieve fast build rates of up to 100  $\text{cm}^3/\text{h}$  but has a large range with speeds as low as 4.2  $\text{cm}^3$ . This is likely due to the number of print parameters which can be altered to increase or decrease the printing rate including using different diameter nozzles. MJ is shown to have the fastest build rate achieving a build rate as high as 147  $\text{cm}^3/\text{h}$ .

MJ is well suited for small to medium-sized batch production of quasi-optical components owing to its high processing rate and capability to produce multiple parts simultaneously. Although VP offers high resolution its relatively slow processing rate is better suited for prototyping.

Although the processing rate of AM systems can be adjusted, higher print speeds on ME systems can impact the optical properties of samples, with faster printing speeds reducing the refractive index and increasing

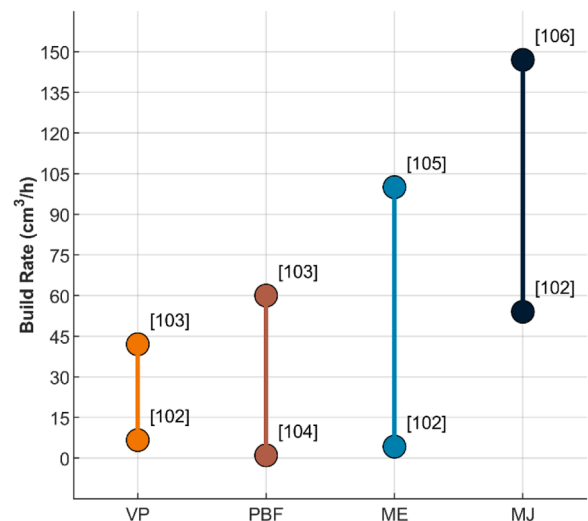


Fig. 14. Range of recorded build rates for AM processes, data obtained from references cited in [102–106].

the absorption coefficient of FFF-printed samples [107]. Variation of the build rate would also likely impact the spectral properties of samples printed using VP and MJ, as the exposure time is a key factor determining their throughput. Shorter exposure times would increase throughput but could reduce the degree of polymerisation, altering the microstructure of cured photopolymers and impacting their optical properties at THz frequencies [64].

### 3.4. Limits to improving the resolution of AM technologies

New AM processes and materials are continuously being developed and improving in resolution. The resolution of more widely available systems may evolve to produce minimum features consistently in the tens of microns scale. Several novel high-resolution AM technologies have emerged which build upon existing AM processes allowing for the manufacture of micro/nanoscale devices [108]. Therefore, it is important to understand the restrictions of conventional AM technologies that prevent them from producing smaller feature sizes. The hardware limits

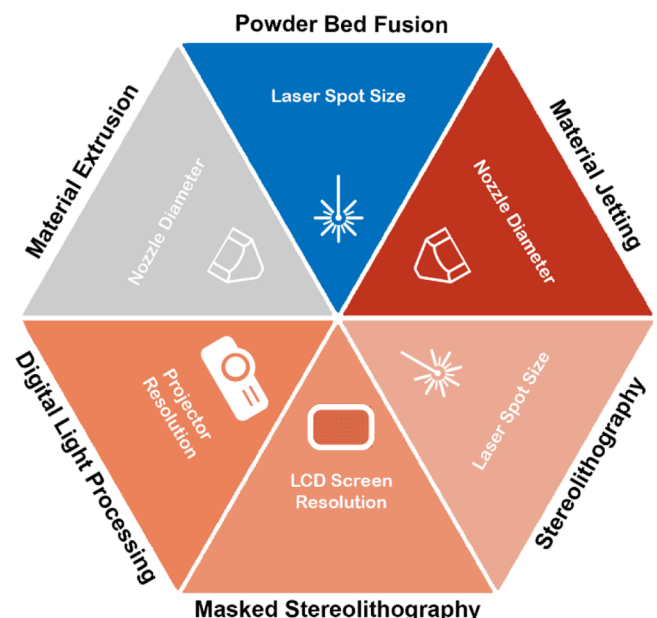


Fig. 15. The hardware limits of AM technologies.

of AM processes are presented in Fig. 15.

The resolution of both ME and MJ is limited by the nozzle diameter used in the process. A smaller diameter allows for thinner layer thicknesses and line widths see Fig. 16(A). FFF is typically limited to a minimum nozzle size of 0.1–0.2 mm with studies showing that diameters below this size have a negative effect on print quality [109]. This occurs as smaller apertures lead to pressure build-ups which result in blockages and reduces flow rates which cause changes in the rheological behaviour of the filament, limiting the achievable resolution of FFF systems [110].

MJ systems use low-viscosity acrylate-based resins, these resins are also often heated further reducing their viscosity [114]. Therefore, reducing the nozzle size has less of an impact allowing the use of nozzles

with apertures of 50  $\mu\text{m}$  [115], allowing MJ to achieve smaller minimum feature sizes than FFF.

Laser-based AM processes including SLS, SLM and SLA are limited in terms of resolution by the size of the laser spot. A reduction in the laser spot size allows for the creation of smaller minimum feature sizes and increases the x and y resolution of printed parts [116].

The resolution of Masked Stereolithography (MSLA) and Digital Light Processing (DLP) systems is determined by the pixel resolution of the screen/projector installed. Replacing a 2 K screen with a 4 K screen can increase the x/y printing resolution of an MSLA system by up to 10  $\mu\text{m}$  [117]. The resolution of these processes has continually improved with each new model, MSLA screen resolutions have improved from 2 K

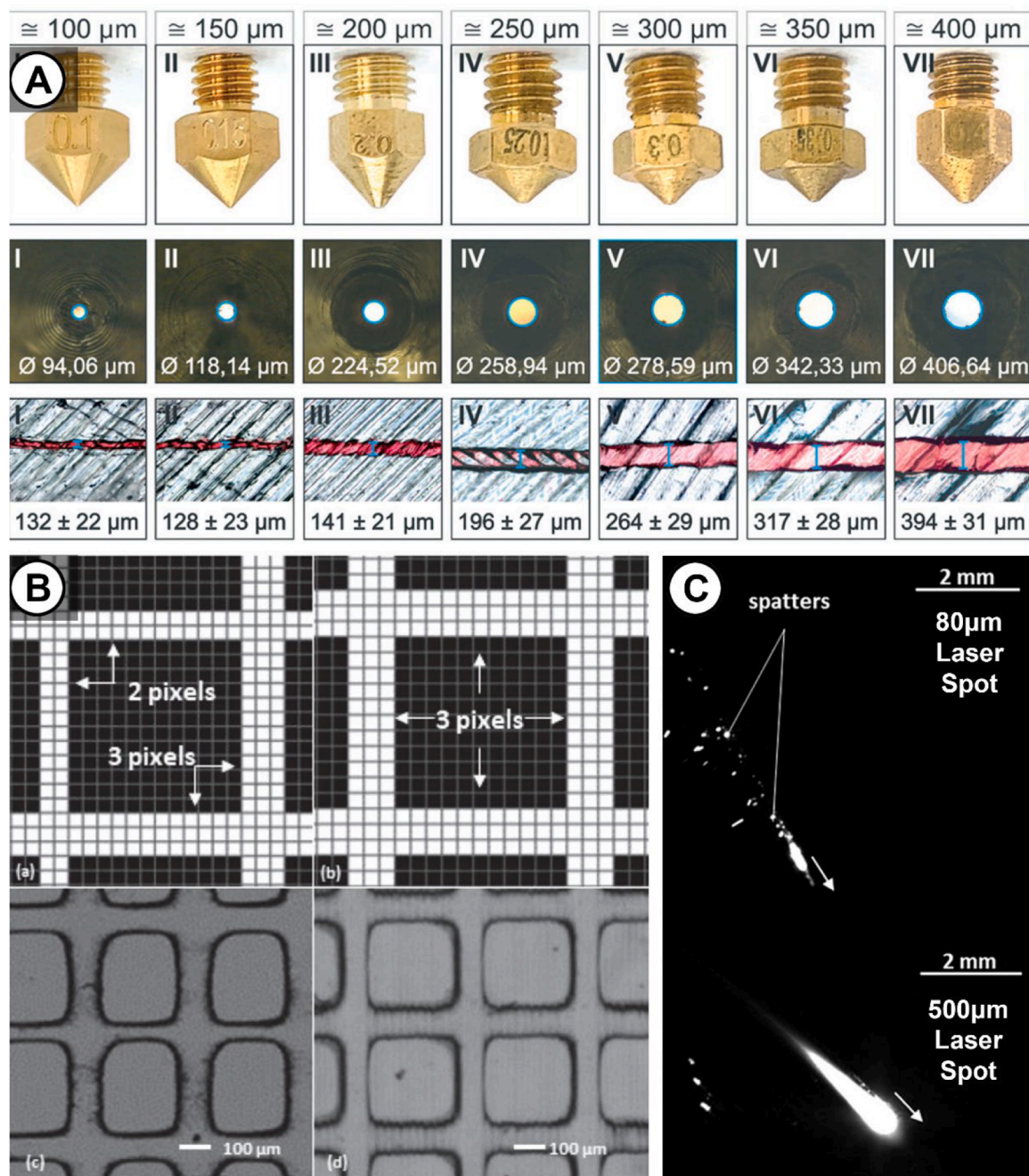


**Fig. 16.** (A) Comparison of different nozzle diameters showing microscopy images of the nozzle orifices and the microchannel obtained with each nozzle diameter. Reproduced with permission [111]. Copyright 2021, Royal Society of Chemistry. (B) MSLA line width adjustment by pixel length. Reproduced under terms of the CC-BY license [112]. Copyright 2022, Zuchowicz et al., published by MDPI. (C). L-PBF laser spot size comparison. Reproduced with permission [113]. Copyright 2020, Elsevier.

to 4 K with more recent models having 8 K screens [112].

VP processes including laser and screen-based processes are shown to be less restricted in achieving higher resolutions, with manufacturers improving the resolution of these processes with each new model. In future MSLA systems may be installed with higher resolution screens. Nozzle based processes are more restricted owing to the complications of using smaller nozzle orifices and the effect it can have on the printing process. Future advancements in AM technologies increasing their resolution could enable the fabrication of high-value THz optical components on low-cost desktop AM systems, improving the surface finish and geometric accuracy of 3D printed optics.

### 3.5. Advanced AM processes capable of producing THz devices

Although the review has identified some commercially available AM technologies which can create minimum feature sizes compatible with THz wavelengths, these systems would struggle to produce quasi-optical components operational at the upper end of the THz spectrum. These frequencies require minimum feature sizes in the scale of tens of microns [118]. Therefore, it is important to consider the potential of more advanced AM technologies for the manufacture of high-frequency THz devices.

Conventional micro and nano-fabrication processes, such as micro-machining, lithography, and microforming are highly precise, yet they are limited in their ability to manufacture complex 3D geometries. These techniques struggle to produce high-aspect-ratio structures and complex geometric features such as conical spirals and polyhedral shapes [119]. Additionally, they have a limited material library and processing capacity [120]. These restrictions limit the types of quasi-optical designs

that can produced with conventional techniques, with advanced AM techniques providing a potential solution to manufacture complex 3D geometries at the nano and micro scale.

Aerosol Jet Printing (AJP), Direct Ink Writing (DIW), Two-Photon Polymerization (TPP) and forms of Electrohydrodynamic (EHD) 3D printing have all been identified as high-precision AM processes well suited to produce micro and nanoelectronics [121]. Diagrams of the EHD, AJP and TPP processes are shown in Fig. 17.

Although AJP, DIW and EHD propel material through a nozzle they can achieve higher resolutions than other nozzle-based AM technologies such as ME and MJ. Typically, these advanced processes use low-viscosity materials typically inks/gels which allows for nozzles with smaller apertures to be used [122]. There are examples of DIW using nozzle sizes as low as 50  $\mu\text{m}$  [123]. Both AJP and EHD printing techniques propel material through a nozzle at a smaller diameter than the nozzles orifice achieving a higher print resolution.

AJP does this by using a carrier and sheath gas to transport droplets of a material. The sheath gas focuses the droplets into a beam with a diameter below the size of the nozzle's orifice [124].

EHD printing processes require high voltages to generate powerful electric fields which control depositions from a nozzle. The electric field draws material from the nozzle creating a Taylor's cone with extruded material having a diameter smaller than the nozzle size [125]. The EHD technique is often hybridised with another AM process for example EHD FFF (E-FFF) to improve the resolution of the technology [126].

TPP is an advanced form of VP and is well-established as a method for micro/nanofabrication [127]. Unlike SLA, which is limited in terms of resolution by the laser spot size, TPP uses a femtosecond laser. This laser creates short pulses which penetrate the resin bath with the pulses

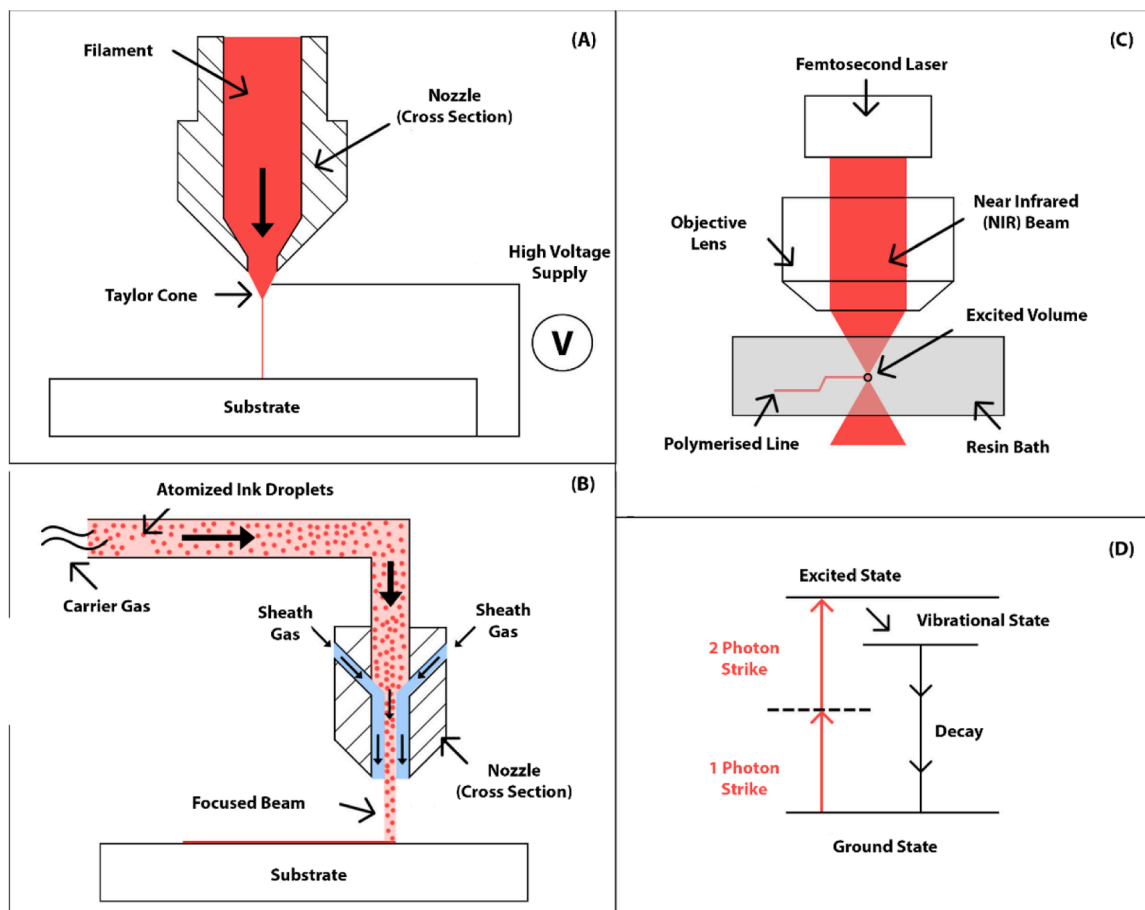


Fig. 17. (A) Electrohydrodynamic 3D printing diagram. (B) Aerosol Jet printing diagram. (C) Two-Photon Polymerization instrumentation. (D) Two-Photon Polymerization process.

working to excite the photopolymer, triggering polymerization in an extremely localized volume [128].

To indicate the resolution of these advanced processes several studies were analysed to investigate the record printable line widths see Fig. 18.

As shown TPP can print extremely small line widths as low as 80 nm, surpassing the resolution of other more common VP technologies. However, this level of resolution is considerably below the wavelength scale of the THz band, being better suited for producing meta surfaces which feature unique optical properties [129].

Electrohydrodynamic FFF far exceeds the resolution of standard FFF systems being able to print line widths as low as 20  $\mu\text{m}$ . AJP and DIW also printed at high resolutions producing line widths of 20  $\mu\text{m}$  and 50  $\mu\text{m}$ , respectively.

Although the minimum feature size and line width have different meanings they are related, these line widths values are far below what is achievable with more common forms of AM showing their potential to fabricate high-resolution structures needed for high-frequency applications.

The applications for these technologies exploit their high resolution, with their being example applications in the biomedical field [133] and increasingly in the electronics industry for micro and nanoelectronics [121]. A comprehensive literature search revealed that there are few examples of their use to produce components for THz applications, with AJP being used as a method to coat 3D printed components operating at THz frequencies [134]. This is likely owing to these processes being more experimental and highly specialised. The capital equipment costs of some of these processes also limit access to them with TPP systems costing over \$100,000 in 2017 [135]. VP and ME systems are more affordable as patents for these technologies have expired decreasing the price significantly.

Recent studies have identified TPP's potential for producing THz components due to its sub-micron resolution however, compatible photopolymers are shown to be absorptive at high frequencies [70].

#### 4. Evaluation of AM processes to produce THz optics

The review has investigated the optical properties of AM materials at THz frequencies. It has also analysed the process characteristics of a range of AM technologies and assessed their suitability to produce quasi-optical components.

Although several advanced technologies were investigated, this was to show the upper limits AM can achieve in terms of resolution. These

highly precise technologies are typically suited to high-value or large-scale manufacturing and are less accessible and expensive to purchase. They also have their own drawbacks which rule them out, for example, TPP is shown to have a slow build rate and therefore would not be suitable for mass or even medium-sized batch manufacturing. Therefore, the focus of the discussion will be on more accessible AM technologies.

An evaluation of ME, VP, MJ and PBF was undertaken using data obtained throughout the review to assess their suitability to fabricate THz optics, see Fig. 19. To classify the technologies, they were scored against five factors, see Table 2. Midpoints of data ranges were used to calculate the mean.

The following criteria were used to score processes based on their suitability to produce quasi-optical components:

1. Mean minimum feature size: Processes capable of producing smaller feature sizes received higher scores.

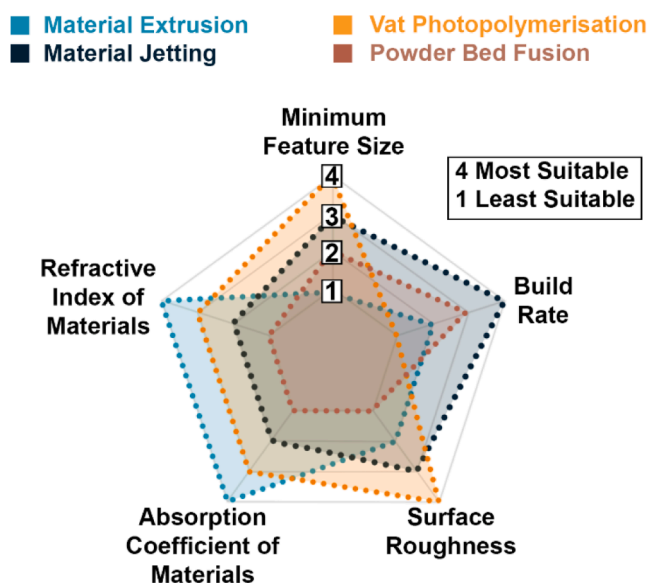


Fig. 19. Suitability of different AM-processes to manufacture quasi-optical components.

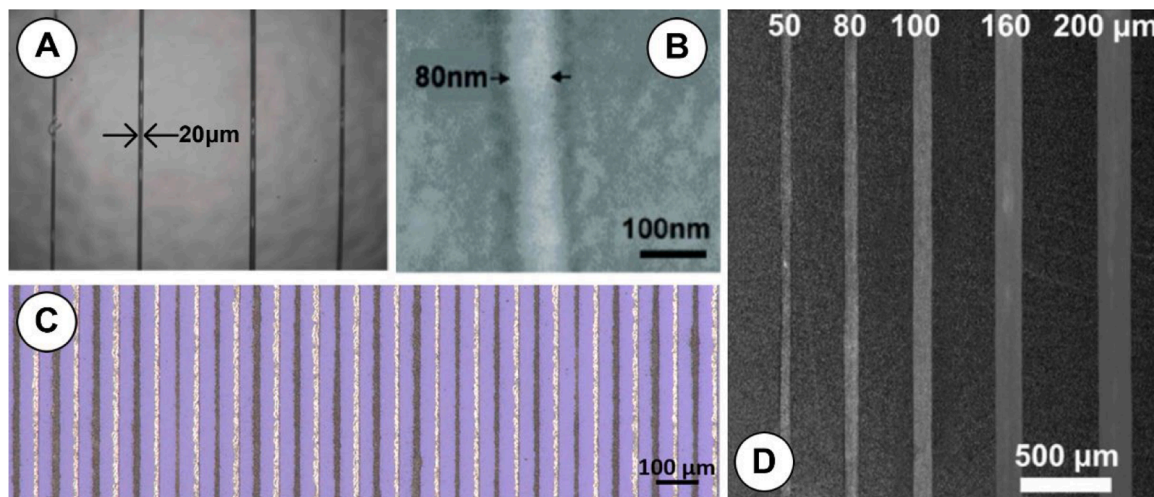


Fig. 18. (A). Electrohydrodynamic jet FFF printed sample. Adapted with permission, scale indicator added [126]. Copyright 2016, IOP Science. (B). SEM Images of 80 nm polymer lines made using TPP. Reproduced with permission [130]. Copyright 2007, AIP Publishing. (C). Aerosol Jet printed line array 20  $\mu\text{m}$  linewidth. Reproduced with permission [131]. Copyright 2018, IOP Science. (D). DIW-printed silver line array. Reproduced with permission [132]. Copyright 2023, ACS Publications.

**Table 2**  
Scoring of AM processes based on suitability to manufacture THz devices.

Process	Refractive Indices (Range Value at 1 THz)	Absorption Coefficients (Lowest Value at 1 THz)	Mean Minimum Feature Size ( $\mu\text{m}$ )	Mean Surface Roughness ( $\mu\text{m}$ )	Mean Build Rate ( $\text{cm}^3/\text{h}$ )
Material Extrusion	.31	1	415.17	12.09	28.74
Material Jetting	.03	24	182.42	5.67	87.45
Vat Photopolymerization	.11	19	80.75	1.42	24.03
Powder Bed Fusion	N/A	N/A	270.67	14.76	29.82

2. Mean build rate: A higher processing rate was scored more favourably.
3. Mean Surface Roughness: Processes that produced smoother surfaces received higher scores.
4. Minimum absorption coefficient at 1 THz: Higher scores were awarded based on the ability to print transparent materials.
5. Refractive index range at 1 THz: High scores were awarded based on the ability to print materials with a larger range of refractive indices.

To reduce loss, optical components require highly transparent materials. Therefore, materials are chosen with a low absorption coefficient for the target frequency of the optic. VP, MJ and PBF were shown to have a material library primarily consisting of materials with a high absorption coefficient  $>15 \text{ cm}^{-1}$  at 1 THz. Alternatively, ME can print using a range of filaments, including some non-polar polymers (HDPE and PS) which are highly transparent in the THz region.

A moderate to high refractive index ( $n = >1.55$ ) is also desirable for THz lenses allowing for more efficient manipulation of THz waves, with higher refractive indices allowing for lenses which are thinner and have a shorter focal length. ME has been shown to print materials with refractive indices ranging from 1.48 to 1.70. However, although both Nylon and PVA filaments have a high refractive index and are compatible with ME, they are both polar polymers which are highly absorptive in the THz region. The refractive index of photopolymers compatible with MJ and VP were more limited, ranging from 1.61 to 1.72 at 1 THz.

Smooth surfaces comparable to the operational wavelength of the lens are also required to reduce loss through diffuse scattering. ME and PBF were shown to produce surfaces with roughness average values comparable to  $\lambda/20$  for 1 THz (15  $\mu\text{m}$ ). However, optics manufactured using PBF or ME operational beyond  $>1$  THz would be more likely to experience loss due to the shortening of the wavelength. Both VP and MJ were shown to be capable of producing smoother surfaces than ME and PBF, with roughness averages comparable to the  $\lambda/20$  for 10 THz (1.5  $\mu\text{m}$ ).

The build rates of AM processes were also investigated, although the build rate is not a critical factor in the production of quasi-optical components, a faster build rate allows for more scalable production. MJ was shown to highest processing rate, with a mean build rate of 87.5  $\text{cm}^3/\text{h}$ , being well suited for small to medium-sized batch production. ME, PBF and VP were shown to have a lower processing rate and would be better suited for the manufacture of small batches or individual components.

As shown, there are trade-offs between the various process categories with advantages and disadvantages to producing THz optical components with each. The choice of AM process will be highly dependent on the requirements of the quasi-optical component and its desired properties.

## 5. Potential areas for future investigation

The review has uncovered several areas that would be fruitful to explore through new research.

### 5.1. THz characterisation with standardised AM parameters

One avenue would be to repeat some of the identified experiments investigating the properties of AM materials at THz frequencies. The review collected results from multiple sources with materials samples being manufactured using different AM systems and models. As discussed, any adjustments to the build parameters on an AM system can alter the material's properties, another consideration is that different systems have varying levels of build quality. Repeating the experiments with a set of standardised parameters on the same printer would provide a more accurate comparison of the properties of AM materials at THz frequencies.

Additionally, research has demonstrated that optimisation of AM parameters can lead to a significant change in the properties of AM materials at THz frequencies. Further research should expand on this showcasing what is achievable and investigating the limits of this relationship.

Further characterization of AM materials would also be beneficial to the field. As the number of materials available for AM systems is continuously growing further investigation of new materials with wider-ranging properties could enhance the appeal of 3D printing for THz applications. Promising materials are shown to be ceramics as they have desirable properties for optical devices.

The spectral properties of AM materials beyond 1 THz are largely unknown, with few studies conducting material characterisation at these higher frequencies. Characterisation of materials above 1 THz could identify the vibrational modes and the unique spectral features of AM materials at higher frequencies, determining their suitability to be used for quasi-optical components across an extended bandwidth.

### 5.2. THz characterisation of photopolymer composites

Although the properties of 3D-printed composites have been investigated, the focus of this work has been on filaments compatible with ME. Although filaments have wide-ranging properties ME does not have the required resolution for fabricating THz optics with a target frequency  $>1$  THz. Further investigation of the properties of composite resins compatible with VP could be valuable as this technology offers the resolution needed but is limited by the properties of photopolymer materials with them being absorptive, with composites potentially offering a wider range of material properties.

### 5.3. THz characterisation of absorptive AM materials

The review identified a lack of research on the properties of materials compatible with PBF and other metal AM technologies. These materials would likely be unsuitable for refractive lenses and other low-loss THz components due to metals and polar polymers being absorptive to THz radiation. However, they may possess desirable properties, including a high refractive index and a high degree of reflectivity, suitable for THz mirrors.

### 5.4. Comparison of AM and conventionally manufactured quasi-optics

As discussed throughout the review, research primarily focuses on

the THz characterisation of AM materials and the demonstration of 3D-printed quasi-optical components. However, it would be beneficial to compare the performance of 3D-printed components against conventionally manufactured optics to assess their potential. As highlighted in the review, 3D-printed components can contain voids and pores within their structure, and their surfaces can also have high levels of roughness. These imperfections may reduce the performance of 3D printed optics, unlike moulded alternatives which have smooth surfaces and significantly lower porosity. There may also be variations between batches of 3D-printed components, requiring a robust quality control process to validate printed quasi-optics.

## 6. Conclusion

The review investigated the potential of additive manufacturing to produce the next generation of THz quasi-optical components. It has been shown that several additive processes can print minimum feature sizes under 100  $\mu\text{m}$  and can produce surfaces smooth in relation to the wavelength of the THz region (1–10 THz). Some of these technologies have also developed to now be low-cost and easily accessible.

However, a trade-off between resolution and material properties has been identified. High-resolution additive processes, such as vat photopolymerization, have a limited material choice owing to photopolymer resins being absorptive and having a relatively low refractive index at THz frequencies. In contrast, lower-resolution processes, including material extrusion, have a wider material library which includes non-polar polymers which are highly transparent in the THz region. However, the process does not have the necessary resolution to produce feature sizes and surface finishes comparable to the wavelengths in the THz region, which are required for THz optics.

Optics fabricated using high-resolution techniques may be inefficient owing to the use of absorptive materials. Whereas low-resolution techniques may produce optics which experience attenuation losses due to poor geometric accuracy and high surface roughness.

3D printed composites and ceramics are a possible solution to widen the range of material properties. These materials could allow for the production of THz lenses which absorb less THz radiation, are thinner and have a shorter focal distance.

Further characterisation of the optical properties of AM materials at THz frequencies is required to showcase which processes would be more suitable for various quasi-optical designs. A better understanding of the properties of AM materials beyond 1 THz is also needed, with most examples characterising the properties around or below 1 THz.

## Appendix A. Collected data of the refractive indices of AM materials

(Table 3).

**Table 3**

The recorded refractive index ( $n$ ) of 3D printed samples made from various AM materials at 1 THz.

Material Name	AM Material Group	$n$ at 1 THz	References
PP	Filament (FFF)	1.48	[24]
HIPS	Filament (FFF)	1.49	[7]
HDPE	Filament (FFF)	1.53	[14]
Cyclic Olefin Copolymer (TOPAS)	Filament (FFF)	1.53	[44]
ASA	Filament (FFF)	1.54	[45]
PS	Filament (FFF)	1.56	[14]
ABS	Filament (FFF)	1.57	[14]
PLA Wood	Composite Filament (FFF)	1.59	[24]
PET-G	Filament (FFF)	1.6	[7]
HTM140 V2	Photopolymer (VP)	1.61	[15]
Peopoly Grey UV Resin	Photopolymer (VP)	1.61	[45]
TPU	Filament (FFF)	1.62	[45]
Formlabs Gray Resin	Photopolymer (VP)	1.62	[15]

(continued on next page)

## Permission to reproduce material from other sources

Appropriate permissions to reproduce material from the following sources has been obtained:

- American Chemical Society (ACS Publications) (Fig. 18d)
- American Institute of Physics (AIP Publishing) (Fig. 18b)
- Elsevier (Fig. 16c)
- Institute of Physics (IOP Science) (Fig. 18a & 18c)
- Optica (Fig. 1d)
- Royal Society of Chemistry (Fig. 16a)
- Springer Nature (Fig. 1a)

Additionally, some material has been reproduced under the Creative Commons Attribution 4.0 International License (CC-BY 4.0) from the following sources:

- Institute of Electrical and Electronics Engineers Access (IEEE Access) (Fig. 1b)
- Scientific Reports (Fig. 1c)
- Multidisciplinary Digital Publishing Institute (MDPI) (Fig. 16b)

## CRediT authorship contribution statement

**Luke Phillips:** Writing – original draft, Visualization, Methodology. **Alexander Valavanis:** Writing – review & editing, Supervision, Funding acquisition. **Andrew D. Burnett:** Writing – review & editing, Supervision. **Robert Kay:** Writing – review & editing, Supervision, Conceptualization. **Russell Harris:** Writing – review & editing, Supervision, Conceptualization. **Ehab Saleh:** Writing – review & editing, Supervision, Conceptualization.

## Declaration of competing interest

The authors declare that they have no known competing financial interests or personal relationships that could have appeared to influence the work reported in this paper.

## Funding statement

The authors gratefully acknowledge financial support from UK Research and Innovation (Future Leader Fellowship MR/S016969/1 and MR/Y011775/1) and a Doctoral Scholarship from The School of Mechanical Engineering, University of Leeds, U.K.

Table 3 (continued)

Material Name	AM Material Group	$n$ at 1 THz	References
Formlabs Clear Resin	Photopolymer (VP)	1.635	[47]
PLA	Filament (FFF)	1.64	[24]
PC	Filament (FFF)	1.64	[24]
BVOH	Filament (FFF)	1.64	[24]
ABS Flex Black	Photopolymer (VP)	1.64	[15]
RGD450	Photopolymer (MJ)	1.66	[15]
ABS Tough	Photopolymer (VP)	1.66	[15]
Phrozen Clear	Photopolymer (VP)	1.66	[48]
Co-Polyester	Filament (FFF)	1.67	[46]
VeroBlue RGD240	Photopolymer (MJ)	1.69	[47]
Photosilver	Photopolymer (VP)	1.69	[15]
Unspecified UV Resin	Photopolymer (VP)	1.70	[49]
Nylon	Filament (FFF)	1.71	[14]
RC-90	Photopolymer (VP)	1.72	[15]
PVA	Filament (FFF)	1.79	[7]
PLA Cu	Composite Filament (FFF)	1.79	[45]
PLA Stone	Composite Filament (FFF)	1.8	[24]
PLA Metal	Composite Filament (FFF)	2.1	[24]
PLA Conductive	Composite Filament (FFF)	2.38	[45]
Alumina	Ceramic Composite (VP)	3.9	[26]

## Appendix B. Collected data of the absorption coefficients of AM materials

(Table 4)

Table 4

The recorded absorption coefficient ( $\alpha$ ) of 3D printed samples made from various AM materials at 1 THz.

Material Name	AM Material Group	Absorption Coefficient ( $\text{cm}^{-1}$ ) at 1 THz	References
COC (TOPAS)	Filament (FFF)	1	[53]
HDPE	Filament (FFF)	1.20	[45]
PS	Filament (FFF)	3	[53]
HIPS	Filament (FFF)	5	[7]
Co-Polyester	Filament (FFF)	8	[46]
PC	Filament (FFF)	10	[7]
ABS	Filament (FFF)	16	[53]
PP	Filament (FFF)	18	[7]
Gray Resin	Photopolymer (VP)	19	[15]
ASA	Filament (FFF)	20.2	[45]
ABS Tough	Photopolymer (VP)	20.5	[15]
HTM140 V V2	Photopolymer (VP)	21	[15]
Phrozen Clear	Photopolymer (VP)	21.1	[48]
RC-70	Photopolymer (VP)	21.75	[15]
Photosilver	Photopolymer (VP)	22.5	[15]
ABS Flex Black	Photopolymer (VP)	22.6	[15]
PET-G	Filament (FFF)	23	[7]
Peopoly Grey	Photopolymer (VP)	23.3	[45]
RGD450	Photopolymer (MJ)	24	[15]
VeroBlue RGD240	Photopolymer (MJ)	(Converted value) 25	[47]
Formlabs Clear	Photopolymer (VP)	(Converted value) 27	[47]
PLA	Filament (FFF)	27	[53]
TPU	Filament (FFF)	29.3	[45]
PVA	Filament (FFF)	30.6	[45]
Nylon	Filament (FFF)	32	[7]
PLA Cu	Composite Filament (FFF)	38.4	[45]
PLA Conductive	Composite Filament (FFF)	255	[45]

## Appendix C. Existing research characterising composites at THz frequencies

(Tables 5, 6)

Table 5

Refractive indices of various composite materials at 1 THz.

Composite	$n$ at 1 THz	References
PDMS + PTFE wt%	PDMS = 1.501 10 % PTFE = 1.515 20 % PTFE = 1.512 40 % PTFE = 1.498	[66]

(continued on next page)

Table 5 (continued)

Composite	$n$ at 1 THz	References
PDMS + Alumina wt%	PDMS = 1.501 10 % Alumina = 1.557 20 % Alumina = 1.6 40 % Alumina = 1.681	[66]
PVC + PS wt%	100 % PVC = 1.663 25 % PS = 1.652 50 % PS = 1.634 75 % PS = 1.617 100 % PS = 1.592	[67]
PLA + Quartz	(1THz) PLA = 1.58 Quartz =1.96 10 % Quartz = 1.59 20 % Quartz = 1.61 30 % Quartz = 1.63 40 % Quartz = 1.65 50 % Quartz = 1.67	[48]
PA + Quartz	(1THz) PA = 1.60 Quartz =1.96 10 % Quartz = 1.60 20 % Quartz = 1.62 30 % Quartz = 1.62 40 % Quartz = 1.64 50 % Quartz =1.65	[48]
UV Resin + Quartz	(1THz) Resin=1.66 Quartz =1.96 10 % Quartz =1.64 20 % Quartz = 1.61 30 % Quartz = 1.57 40 % Quartz = 1.61 50 % Quartz = 1.66	[48]
PS + Wood Powder	(1THz) PS=1.56 10 % WP=1.59 20 % WP=1.6 30 % WP=1.627 40 % WP=1.656 50 % WP=1.676	[29]
PP + Wood Powder	(1THz) PP=1.48 10 %=1.50 20 %=1.53 30 %=1.55 40 %=1.57 50 %=1.60	[29]
ABS + Rice Husk Ash (SiO <sub>2</sub> )	(1THz) ABS=1.56 10 %RHA=1.578 40 %RHA=1.605 50 %RHA=1.601	[68]
PE + TiO <sub>2</sub>	(1THz) PE = 1.6 20 % = 1.7 40 % = 1.81 60 % = 2.12 80 % = 2.96	[65]

Table 6

Absorption coefficients of various composite materials at 1 THz.

Composite	Absorption Coefficient (cm <sup>-1</sup> ) at 1THz	References
PDMS + PTFE wt%	0 % =17.63 10 % =17.55 20 % =16.05 40 % = 15.23	[66]
PDMS + Alumina wt%	0 % = 18.69 20 % =18.31 40 % =17.59	[66]

(continued on next page)

Table 6 (continued)

Composite	Absorption Coefficient ( $\text{cm}^{-1}$ ) at 1THz	References
PS + PVC wt%	0 % =10.4	[67]
	50 % =14.9	
	75 % = 17.72	
PLA + Quartz wt%	PLA = 19.27	[48]
	Quartz=5	
	10 % Quartz = 18.65	
	20 % Quartz = 16.94	
	30 % Quartz = 15.50	
	40 % Quartz = 14.58	
PA + Quartz wt%	50 % Quartz = 12.30	[48]
	PA = 20.41	
	Quartz=5	
	10 % Quartz = 17.13	
	20 % Quartz = 16.75	
	30 % Quartz = 15.53	
UV Resin + Quartz wt%	40 % Quartz = 15.19	[48]
	50 % Quartz = 12.42	
	Resin=21.09	
	Quartz=5	
	10 % Quartz =19.37	
	20 % Quartz = 19.92	
PS + Wood Powder wt%	30 % Quartz = 17.99	[48]
	40 % Quartz = 14.28	
	50 % Quartz = 12.18	
	PS=4.6	
	10 % WP=8.7	
	20 % WP=10.9	
PP + Wood Powder wt%	30 % WP=13.58	[29]
	40 % WP=16.3	
	50 % WP=19	
	10 % WP=5.11	
	20 % WP=8.21	
	30 % WP=10.7	
ABS + Rice Husk Ash (SiO <sub>2</sub> )	40 % WP=12.72	[29]
	50 % WP=15	
	60 % WP = 17	
	ABS =12.72	
	10 %RHA=9.79	
	20 %RHA=8.57	
PE + TiO <sub>2</sub>	30 %RHA=8.94	[68]
	40 %RHA=8.14	
	50 %RHA=7.96	
	PE =0.18	
	40 %=3.15	
	80 %=11.5	[65]

#### Appendix D. Collected data of the minimum feature size of AM processes

(Table 7)

**Table 7**  
Recorded feature sizes of AM processes.

Process	Recorded Minimum Feature Size in Microns	References
ME	600	[80]
ME	321–370	[77]
ME	200–400	[79]
MJ	100	[136]
MJ	340	[80]
MJ	50–100	[137]
MJ	42	[79]
MJ	300	[138]
MJ (Polyjet)	205–270	[77]
PBF (DMLS)	381	[139]
PBF (SLM)	140	[139]
PBF (SLS)	500	[80]
PBF (DMLS)	153	[78]
PBF (DMLS)	380	[78]
PBF (SLS)	40–100	[78]
VP (SLA)	94–154	[77]
VP	15–60	[76]
TPP	0.018	[140]
TPP	0.1	[141]

## Appendix E. Surface roughness measurements of AM-produced surfaces

(Table 8)

**Table 8**

Surface roughness measurements of AM-produced surfaces made with various AM process categories.

Process	Roughness Average (Ra)	Material	System	References
Material Extrusion (Top Surface)	0.7–10.5	PLA	Ultimaker 2 +	[86]
Material Extrusion (Side Surface)	4.7–12.8	PLA	Ultimaker 2 +	[86]
Material Extrusion (Top Surface)	2–7	ABS & TPU	Creality CR10	[87]
Material Extrusion (Side Surface)	21–38	ABS & TPU	Creality CR10	[87]
Selective Laser Sintering	13–17	PA12	EOS Formiga P110	[88]
Selective Laser Sintering	14.40–14.62	PA12	EOS Formiga P110	[142]
Material Jetting	0.8–12.99	FullCure 720	Objet 250	[89]
Material Jetting	0.338–8.532	Visijet M2R-WT	MJP2500	[90]
Stereolithography	0.025–2.86	Gray Resin V3	Form 2	[91]
Stereolithography	0.995–1.815	Dental LT Clear	Form 2	[143]

## Appendix F. Collected data of the build rates of AM processes

(Table 9)

**Table 9**

Recorded build rates of AM processes.

Process & Category	Build Rate (cm <sup>3</sup> /h)	References
FFF	10–100	[105]
FFF	4.2–13.2	[102]
FFF	10–80	[144]
FFF	15	[103]
FFF	20	[145]
VP (SLA)	6.6–11.4	[102]
VP (DLP CLIP Carbon 1)	13.8	[146]
VP (DLP CLIP Carbon 2)	41.3	[146]
VP (SLA)	42	[103]
TPP	0.01–0.1	[147]
PBF (SLS)	60	[103]
PBF (SLM)	1–35	[104]
PBF (SLM)	5–50	[104]
PBF (SLM)	1.62–25.92	[148]
MJ	54–69.6	[102]
MJ	69–147	[106]
MJ	75–147	[149]
MJ	69	[150]

## Appendix G. Collected data of the recorded line widths of high-end AM processes

(Table 10)

**Table 10**

Recorded line widths of high-end AM processes.

AM Process	Recorded Line Width	Compatible Materials	References
Two Photon Polymerization (2PP)	100 nano meters	Photopolymers, Photopolymer Composites	[151]
Two Photon Polymerization (2PP)	80 nano meters	Photopolymers, Photopolymer Composites	[130]
Electrohydrodynamic FFF (EFFF)	10 μm	Polymers, Composites	[126]
Aerosol Jet Printing	20–35 μm	Various Inks, Nano particle composite inks	[124]
			[131]
Direct Ink Writing	50 – 200	Polymers, Ceramics, Glass, Metals, Composites	[132]
			[122]

### Data availability

No new data are associated with this article. All data presented in this review are reproduced from their respective references.

### References

- [1] J.S. Rieh, Introduction to terahertz electronics, 2020. [https://books.google.com/books/about/Introduction\\_to\\_Terahertz\\_Electronics.html?id=g5EAEAAAQBAJ](https://books.google.com/books/about/Introduction_to_Terahertz_Electronics.html?id=g5EAEAAAQBAJ) (accessed February 3, 2023).

- [2] I.F. Akyildiz, J.M. Jornet, C. Han, Terahertz band: next frontier for wireless communications, *Phys. Commun.* 12 (2014) 16–32, <https://doi.org/10.1016/J.PHYCOM.2014.01.006>.
- [3] Y.S. Lee, *Principles of Terahertz Science and Technology*, Springer US, Boston, MA, 2009, <https://doi.org/10.1007/978-0-387-09540-0>.
- [4] X.C. Zhang, J. Xu, *Introduction to THz wave photonics*, (2010) 246. [https://books.google.com/books/about/Introduction\\_to\\_THz\\_Wave\\_Photonics.html?id=ErCzAP7Gi\\_OC](https://books.google.com/books/about/Introduction_to_THz_Wave_Photonics.html?id=ErCzAP7Gi_OC) (accessed February 3, 2023).
- [5] A. Kaur, J.C. Myers, M.I.M. Ghazali, J. Byford, P. Chahal, Affordable terahertz components using 3D printing, in: *Proceedings of the Electronic Components and Technology Conference*, 2015, pp. 2071–2076, <https://doi.org/10.1109/ECTC.2015.7159888>, 2015–July.
- [6] J. Sun, F. Hu, Three-dimensional printing technologies for terahertz applications: a review, *Int. J. RF Microw. Comput. Aided Eng.* 30 (2020) e21983, <https://doi.org/10.1002/MMCE.21983>.
- [7] A.D. Squires, R.A. Lewis, Feasibility and characterization of common and exotic filaments for use in 3D printed terahertz devices, *J. Infrared Millim. Terahertz Waves* 39 (2018) 614–635, <https://doi.org/10.1007/s10762-018-0498-y>.
- [8] C. Liu, J. Liu, L. Niu, X. Wei, K. Wang, Z. Yang, Terahertz circular Airy vortex beams, *Sci. Rep.* 7 (2017) 1–8, <https://doi.org/10.1038/s41598-017-04373-6>, 2017 7:1.
- [9] Y. Zhu, T. Tang, S. Zhao, D. Joralmon, Z. Poit, B. Ahire, S. Keshav, A.R. Rajee, J. Blair, Z. Zhang, X. Li, Recent advancements and applications in 3D printing of functional optics, *Addit. Manuf.* 52 (2022), <https://doi.org/10.1016/J.ADDMA.2022.102682>.
- [10] T. Blachowicz, G. Ehrmann, A. Ehrmann, Optical elements from 3D printed polymers, *E-Polymers* 21 (2021) 549–565, <https://doi.org/10.1515/EPOLY-2021-0061>.
- [11] J. Sun, F. Hu, Three-dimensional printing technologies for terahertz applications: a review, *Int. J. RF Microw. Comput. Aided Eng.* 30 (2020), <https://doi.org/10.1002/mmce.21983>.
- [12] F. Cai, Y.H. Chang, K. Wang, C. Zhang, B. Wang, J. Papapolymerou, Low-loss 3-D multilayer transmission lines and interconnects fabricated by additive manufacturing technologies, *IEEE Trans. Microw. Theory Tech.* 64 (2016) 3208–3216, <https://doi.org/10.1109/TMTT.2016.2601907>.
- [13] B. Zhang, Y.X. Guo, H. Zirath, Y.P. Zhang, Investigation on 3-D-printing technologies for millimeter-wave and terahertz applications, *Proc. IEEE* 105 (2017) 723–736, <https://doi.org/10.1109/JPROC.2016.2639520>.
- [14] S.F. Busch, M. Weidenbach, M. Fey, F. Schäfer, T. Probst, M. Koch, Optical properties of 3D printable plastics in the THz regime and their application for 3D printed THz optics, *J. Infrared Millim. Terahertz Waves* 35 (2014) 993–997, <https://doi.org/10.1007/s10762-014-0113-9>.
- [15] N. Duangrit, B. Hong, A.D. Burnett, P. Akkaraekthalin, I.D. Robertson, N. Somjit, Terahertz dielectric property characterization of photopolymers for additive manufacturing, *IEEE Access* 7 (2019) 12339–12347, <https://doi.org/10.1109/ACCESS.2019.2893196>.
- [16] R. Payapullil, L. Zhu, S.H. Shin, M. Stanley, N.M. Ridler, S. Lucyszyn, Polymer-based 3-D printed 140 to 220 GHz metal waveguide thru lines, twist and filters, *IEEE Access* 11 (2023) 32272–32295, <https://doi.org/10.1109/ACCESS.2023.3261241>.
- [17] M. Pérez, D. Carou, E.M. Rubio, R. Teti, Current advances in additive manufacturing, *Procedia CIRP* 88 (2020) 439–444, <https://doi.org/10.1016/J.PROCIR.2020.05.076>.
- [18] A.D. Squires, E. Constable, R.A. Lewis, 3D Printed terahertz diffraction gratings and lenses, *J. Infrared Millim. Terahertz Waves* 36 (2015) 72–80, <https://doi.org/10.1007/S10762-014-0122-8>.
- [19] S. Yang, X. Sheng, G. Zhao, S. Lou, J. Guo, 3D Printed effective single-mode terahertz antiresonant hollow core Fiber, *IEEE Access* 9 (2021) 29599–29608, <https://doi.org/10.1109/ACCESS.2021.3059782>.
- [20] D. Rohrbach, T. Feuer, B.J. Kang, 3D-printed THz wave- and phaseplates, *Opt. Express* 29 (2021) 27160–27170, <https://doi.org/10.1364/OE.433881>. Vol. 29, Issue 17, Pp. 27160-27170.
- [21] V. Ferrando, J.A. Monsoriu, M. Szustakowski, P. Zagrajek, W.D. Furlan, E. Czerwińska, 3D printed diffractive terahertz lenses, *Opt. Lett.* 41 (2016) 1748–1751, <https://doi.org/10.1364/OL.41.001748>. Vol. 41, Issue 8, Pp. 1748-1751.
- [22] J. Neu, C.A. Schmuttenmaer, Tutorial: an introduction to terahertz time domain spectroscopy (THz-TDS), *J. Appl. Phys.* 124 (2018), <https://doi.org/10.1063/1.5047659>.
- [23] L. Liebermeister, S. Nellen, R.B. Kohlhaas, S. Lauck, M. Deumer, S. Breuer, M. Schell, B. Globisch, Terahertz multilayer thickness measurements: comparison of photoelectronic time and frequency domain systems, *J. Infrared Millim. Terahertz Waves* 42 (2021) 1153–1167, <https://doi.org/10.1007/S10762-021-00831-5/TABLES/2>.
- [24] M. Kaluza, M. Surma, P. Komorowski, M. Walczakowski, A. Siemion, THz optical properties of different 3D printing polymer materials in relation to FTIR, Raman, and XPS evaluation techniques, in: *Proceedings of the International Conference on Infrared, Millimeter, and Terahertz Waves, IRMMW*, 2022, <https://doi.org/10.1109/IRMMW-THZ50927.2022.9895845>. THz 2022-August.
- [25] P.D. Cunningham, N.N. Valdes, F.A. Vallejo, L.M. Hayden, B. Polishak, X.H. Zhou, J. Luo, A.K.Y. Jen, J.C. Williams, R. J. Twieg, Broadband terahertz characterization of the refractive index and absorption of some important polymeric and organic electro-optic materials, *J. Appl. Phys.* 109 (2011), <https://doi.org/10.1063/1.3549120>.
- [26] J. Ornik, M. Sakaki, M. Koch, J.C. Balzer, N. Benson, Dielectric properties of 3D printed alumina in the THz range, in: *Proceedings of the International Conference on Infrared, Millimeter, and Terahertz Waves, IRMMW*, 2021, <https://doi.org/10.1109/IRMMW-THZ.2021.9566967>. THz 2021-August.
- [27] S. Wietzke, C. Jansen, M. Reuter, T. Jung, D. Kraft, S. Chatterjee, B.M. Fischer, M. Koch, Terahertz spectroscopy on polymers: a review of morphological studies, *J. Mol. Struct.* 1006 (2011) 41–51, <https://doi.org/10.1016/J.MOLSTRUC.2011.07.036>.
- [28] M. Naftaly, R. Dudley, Terahertz reflectivities of metal-coated mirrors, *Appl. Opt.* 50 (19) (2011) 3201–3204, <https://doi.org/10.1364/AO.50.003201>. Vol. 50Pp. 3201-3204.
- [29] A. Nakanishi, H. Satozono, Terahertz optical properties of wood–plastic composites, *Appl. Opt.* 59 (4) (2020) 904–909, <https://doi.org/10.1364/AO.379758>. Vol. 59Pp. 904-909.
- [30] D. Headland, H. Ebendorff-Heidepriem, D. Abbott, A. Luiten, M. Webb, W. Withayachumnankul, Analysis of 3D-printed metal for rapid-prototyped reflective terahertz optics, *Opt. Express* 24 (2016) 17384–17396, <https://doi.org/10.1364/OE.24.017384>. Vol. 24, Issue 15, Pp. 17384-17396.
- [31] M. Korpela, N. Riikonen, H. Piili, A. Salminen, O. Nyrhilä, Additive manufacturing-past, present, and the future, technical, economic and societal effects of manufacturing 4.0: automation, adaption and manufacturing in Finland and beyond (2020) 17–41. [10.1007/978-3-030-46103-4\\_2/TABLES/2](https://doi.org/10.1007/978-3-030-46103-4_2/TABLES/2).
- [32] V.E. Rogalin, I.A. Kaplunov, G.I. Kropotov, Optical materials for the THz range, *Opt. Spectrosc.* 125 (2018) 851–863, <https://doi.org/10.1134/S0030400X18120172>.
- [33] Y. Kim, M. Yi, B.G. Kim, J. Ahn, Investigation of THz birefringence measurement and calculation in Al 2O3 and LiNbO3, *Appl. Opt.* 50 (2011) 2906–2910, <https://doi.org/10.1364/AO.50.002906>.
- [34] R. Gente, B. Scherger, M. Koch, Density effects on dielectric properties of polymers and ceramics in the THz regime, in: *Proceedings of the International Conference on Infrared, Millimeter, and Terahertz Waves, IRMMW*, 2012, <https://doi.org/10.1109/IRMMW-THZ.2012.6380346>. THz.
- [35] Y. Liu, P.H. Daum, Relationship of refractive index to mass density and self-consistency of mixing rules for multicomponent mixtures like ambient aerosols, *J. Aerosol Sci.* 39 (2008) 974–986, <https://doi.org/10.1016/J.JAEROSCI.2008.06.006>.
- [36] N. Kocic, M. Wichmann, T. Hochrein, P. Heidemeyer, K. Kretschmer, I. Radovanovic, A.S. Mondol, M. Koch, M. Bastian, Lenses for terahertz applications: development of new materials and production processes, *AIP Conf. Proc.* 1593 (2014) 416–419, <https://doi.org/10.1063/1.4873811>.
- [37] A.L. Stanford, J.M. Tanner, *Light: Geometric Optics*, Academic Press, 1985, <https://doi.org/10.1016/B978-0-12-663380-1.50023-9>.
- [38] N. Kocic, M. Wichmann, T. Hochrein, P. Heidemeyer, K. Kretschmer, I. Radovanovic, A.S. Mondol, M. Koch, M. Bastian, Lenses for terahertz applications: development of new materials and production processes, in: 2014: pp. 416–419. [10.1063/1.4873811](https://doi.org/10.1063/1.4873811).
- [39] T. ki Liu, Permittivity and loss characterization of polymer films for terahertz applications, *Highlights Sci. Eng. Technol.* 15 (2022) 159–168, <https://doi.org/10.54097/hset.v15i.2219>.
- [40] M. Bastian, M. Reuter, S. Chatterjee, T. Jung, S. Wietzke, M. Koch, B. Baudrit, C. Jansen, Terahertz time-domain spectroscopy as a tool to monitor the glass transition in polymers, *Opt. Express* 17 (2009) 19006–19014, <https://doi.org/10.1364/OE.17.019006>. Vol. 17, Issue 21, Pp. 19006-19014.
- [41] M. Mumtaz, M.A. Mahmood, S.D. Khan, M.A. Zia, M. Ahmad, I. Ahmad, Experimental measurement of temperature-dependent Sellmeier coefficients and thermo-optic coefficients of polymers in terahertz spectral range, *Opt. Mater.* 91 (2019) 126–129, <https://doi.org/10.1016/J.OPTMAT.2019.03.006>.
- [42] L. Obersto, M. Bisi, A. Kazempour, A. Steiger, T. Kleine-Ostmann, T. Schrader, Measurement comparison among time-domain, FTIR and VNA-based spectrometers in the THz frequency range, *Metrologia* 54 (2017) 77, <https://doi.org/10.1088/1681-7575/AA54C2>.
- [43] K.N. Murphy, M. Naftaly, A. Nordon, D. Markl, Polymer pellet fabrication for accurate THz-TDS measurements, *Appl. Sci.* 12 (2022) 3475, <https://doi.org/10.3390/AP12073475>, 2022, Vol. 12, Page 3475.
- [44] E. Mavrona, J. Graf, E. Hack, P. Zolliker, Towards high quality 3D printed THz devices with cyclic olefin polymer, in: *Proceedings of the 45th International Conference on Infrared, Millimeter, and Terahertz Waves (IRMMW-THz)*, IEEE, 2020, pp. 1–2, <https://doi.org/10.1109/IRMMW-THz46771.2020.9370782>.
- [45] C.H. Brodie, I. Spotts, H. Reguigui, C.A. Leclerc, M.E. Mitchell, J.F. Holzman, C. M. Collier, Comprehensive study of 3D printing materials over the terahertz regime: absorption coefficient and refractive index characterizations, *Opt. Mater. Express* 12 (2022) 3379, <https://doi.org/10.1364/OME.465820>.
- [46] A.T. Clark, J.F. Federici, I. Gatley, Effect of 3D printing parameters on the refractive index, attenuation coefficient, and birefringence of plastics in terahertz range, *Adv. Mater. Sci. Eng.* 2021 (2021), <https://doi.org/10.1155/2021/8276378>.
- [47] X. Ruan, Chi, H. Chan, C.H. Chan, Terahertz free-space dielectric property measurements using time-and frequency-domain setups, (2019). [10.1002/mmce.21839](https://doi.org/10.1002/mmce.21839).
- [48] H.Y. Peng, Y.A. Wei, Y.C. Hsu, K.C. Lin, P.Y. Yeh, C.S. Yang, C.P. Cheng, Complex optical properties of polymeric composite materials mixed with quartz powder and investigated by THz time-domain spectroscopy, *Opt. Mater. Express* 12 (2022) 22–33, <https://doi.org/10.1364/OME.442626>. Vol. 12, Issue 1, Pp. 22-33.
- [49] M.S. Islam, J. Sultana, C.M.B. Cordeiro, A.L.S. Cruz, A. Dlnoviter, B.W.H. Ng, D. Abbott, Broadband characterization of glass and polymer materials using THz-TDS, in: *Proceedings of the International Conference on Infrared, Millimeter, and Terahertz Waves, IRMMW-THz*, 2019, <https://doi.org/10.1109/IRMMW-THZ.2019.8874013>, 2019-September.

- [50] G. Xu, M. Skorobogatiy, 3D printing technique and its application in the fabrication of THz fibers and waveguides, *J. Appl. Phys.* 133 (2023) 210901, <https://doi.org/10.1063/5.0146054/2894490>.
- [51] F. D'Angelo, M. Bonn, R. Gente, M. Koch, D. Turchinovich, Ultra-broadband THz time-domain spectroscopy of common polymers using THz air photonics, *Opt. Express* 22 (2014), <https://doi.org/10.1364/OE.22.012475>.
- [52] H. Xiao, J. Huang, M. Wang, W. Huang, M. Li, G. Jin, Unraveling molecular loss processes for dielectric polymers in the terahertz frequency range: impact of polarity and chain rigidity, *Polymer* 297 (2024) 126855, <https://doi.org/10.1016/J.POLYMER.2024.126855> (Guildf).
- [53] E. Castro-Camus, M. Koch, A.I. Hernandez-Serrano, Additive manufacture of photonic components for the terahertz band, *J. Appl. Phys.* 127 (2020) 210901, <https://doi.org/10.1063/1.5140270>.
- [54] S. Balzereit, F. Proes, V. Altstädt, C. Emmelmann, Properties of copper modified polyamide 12-powders and their potential for the use as laser direct structurable electronic circuit carriers, *Addit. Manuf.* 23 (2018) 347–354, <https://doi.org/10.1016/J.ADDMA.2018.08.016>.
- [55] D.M. Shah, J. Morris, T.A. Plaisted, A.V. Amirkhizi, C.J. Hansen, Highly filled resins for DLP-based printing of low density, high modulus materials, *Addit. Manuf.* 37 (2021) 101736, <https://doi.org/10.1016/J.ADDMA.2020.101736>.
- [56] G. Taormina, C. Sciancalepore, M. Messori, F. Bondioli, 3D printing processes for photocurable polymeric materials: technologies, materials, and future trends, *J. Appl. Biomater. Funct. Mater.* 16 (2018) 151–160, <https://doi.org/10.1177/2280800018764770>.
- [57] G. McKerricher, M. Vaseem, A. Shamim, Fully inkjet-printed microwave passive electronics, *Microsyst. Nanoeng.* 1 (3) (2017) 1–7, <https://doi.org/10.1038/micronano.2016.75>, 2017 3.
- [58] Formlabs, Safety data sheet gray resin, (2022). <https://formlabs-media.formlabs.com/datasheets/2001046-SDS-ENCA-0.pdf> (accessed September 18, 2023).
- [59] M. Naftaly, G. Savvides, F. Alshareef, P. Flanigan, G. Lui, M. Florescu, R. A. Mullen, Non-destructive porosity measurements of 3D printed polymer by terahertz time-domain spectroscopy, *Appl. Sci.* 12 (2022) 927, <https://doi.org/10.3390/APP12020927>, 2022, Vol. 12, Page 927.
- [60] J. Brackett, D. Cauthe, J. Condon, T. Smith, N. Gallego, V. Kunc, C. Duty, The impact of infill percentage and layer height in small-scale material extrusion on porosity and tensile properties, *Addit. Manuf.* 58 (2022) 103063, <https://doi.org/10.1016/J.ADDMA.2022.103063>.
- [61] P.H.M. Cardoso, R.R.T.P. Coutinho, F.R. Drummond, M. do N. da Conceição, R. M. da SM Thiré, Evaluation of printing parameters on porosity and mechanical properties of 3D printed PLA/PBAT blend parts, *Macromol. Symp.* 394 (2020) 2000157, <https://doi.org/10.1002/MASY.202000157>.
- [62] Y. AbouelNour, N. Gupta, *In-situ* monitoring of sub-surface and internal defects in additive manufacturing: a review, *Mater. Des.* 222 (2022) 111063, <https://doi.org/10.1016/J.MATDES.2022.111063>.
- [63] A. Oleff, B. Küster, M. Stonis, L. Overmeyer, Process monitoring for material extrusion additive manufacturing: a state-of-the-art review, *Prog. Addit. Manuf.* 6 (4) (2021) 705–730, <https://doi.org/10.1007/S40964-021-00192-4>, 20216.
- [64] D. Jang, S. Lee, H. Ryu, E.Y. Rho, J. Kim, M. Seo, T.D. Lee, S. Lee, Terahertz refractive index control of 3D printing materials by UV exposure, *Opt. Commun.* 575 (2025) 131262, <https://doi.org/10.1016/J.OPTCOM.2024.131262>.
- [65] C. Dubois, A. Dupuis, M. Skorobogatiy, B. Ung, K. Stoeffler, High-refractive-index composite materials for terahertz waveguides: trade-off between index contrast and absorption loss, *J. Opt. Soc. Am. B* 28 (4) (2011) 917–921, <https://doi.org/10.1364/JOSAB.28.000917>, Vol. 28Pp. 917-921.
- [66] D. Headland, P. Thurgood, D. Stavrevski, W. Withayachumnankul, D. Abbott, M. Bhaskaran, S. Sriram, Doped polymer for low-loss dielectric material in the terahertz range, *Opt. Mater. Express* 5 (2015) 1373, <https://doi.org/10.1364/OME.5.001373>.
- [67] N. Farman, M. Mumtaz, M.A. Mahmood, S.D. Khan, M.A. Zia, M. Raffi, M. Ahmed, I. Ahmad, Investigation of optical and dielectric properties of polyvinyl chloride and polystyrene blends in terahertz regime, *Opt. Mater.* 99 (2020) 109534, <https://doi.org/10.1016/J.OPTMAT.2019.109534> (Amst).
- [68] H.Y. Peng, C.S. Yang, Y.A. Wei, Y.C. Ruan, Y.C. Hsu, C.F. Hsieh, C.P. Cheng, Terahertz complex refractive index properties of acrylonitrile butadiene styrene with rice husk ash and its possible applications in 3D printing techniques, *Opt. Mater. Express* 11 (2021) 2777–2786, <https://doi.org/10.1364/OME.433534>, Vol. 11, Issue 9, Pp. 2777-2786.
- [69] A. Malas, D. Isakov, K. Couling, G.J. Gibbons, Fabrication of high permittivity resin composite for Vat photopolymerization 3D printing: morphology, thermal, dynamic mechanical and dielectric properties, *Materials* 12 (2019) 3818, <https://doi.org/10.3390/MA12233818>, 2019, Vol. 12, Page 3818.
- [70] E.; Magaway, Y.; Farahi, S.M.; Hanham, J.; Zhang, A.; Guaidia-Moreno, M. Navarro-Cia, Silica nanoparticle-based photoresin for THz high-resolution 3D microfabrication by two-photon polymerization, (2023). [10.1109/THZ.2023.3275282](https://doi.org/10.1109/THZ.2023.3275282).
- [71] Y. Lakhdar, C. Tuck, J. Binner, A. Terry, R. Goodridge, Additive manufacturing of advanced ceramic materials, *Prog. Mater. Sci.* 116 (2021) 100736, <https://doi.org/10.1016/J.PMATSCI.2020.100736>.
- [72] S. Zakeri, M. Vippola, E. Levänen, A comprehensive review of the photopolymerization of ceramic resins used in stereolithography, *Addit. Manuf.* 35 (2020) 101177, <https://doi.org/10.1016/J.ADDMA.2020.101177>.
- [73] B. Zhang, W. Chen, Y. Wu, K. Ding, R. Li, Review of 3D printed millimeter-wave and terahertz passive devices, *Int. J. Antennas Propag.* 2017 (2017), <https://doi.org/10.1155/2017/1297931>.
- [74] M.J. Fitch, R. Osiander, Terahertz waves for communications and sensing, *Johns Hopkins APL Tech. Dig.* 25 (2004). <http://www.ntia.doc.gov/osmhome/allochrt.pdf>, accessed April 6, 2023.
- [75] D. Headland, W. Withayachumnankul, M. Webb, H. Eberdorff-Heidepriem, A. Luiten, D. Abbott, Analysis of 3D-printed metal for rapid-prototyped reflective terahertz optics, *Opt. Express* 24 (2016) 17384, <https://doi.org/10.1364/OE.24.017384>.
- [76] T. Zandrini, S. Florczak, R. Levato, A. Ovsianikov, Breaking the resolution limits of 3D bioprinting: future opportunities and present challenges, *Trends Biotechnol.* (2022), <https://doi.org/10.1016/J.TIBTECH.2022.10.009>.
- [77] N.P. Macdonald, J.M. Cabot, P. Smejkal, R.M. Guijt, B. Paull, M.C. Breadmore, Comparing microfluidic performance of three-dimensional (3D) printing platforms, *Anal. Chem.* 89 (2017) 3858–3866, <https://doi.org/10.1021/ACS.ANALCHEM.7B00136>.
- [78] S.Y. Chin, V. Dikshit, B.M. Priyadarshini, Y. Zhang, Powder-based 3D printing for the fabrication of micro and mesoscale features, *Micromachines* 11 (2020) 658, <https://doi.org/10.3390/M111070658>, 2020, Vol. 11, Page 658.
- [79] R. Bahr, B. Tehrani, M.M. Tentzeris, Exploring 3-D printing for new applications, *IEEE Microw. Mag.* 19 (2018) 57–66, <https://doi.org/10.1109/MMM.2017.2759541>.
- [80] B. Bhushan, M. Caspers, An overview of additive manufacturing (3D printing) for microfabrication, *Microsyst. Technol.* 23 (2017) 1117–1124, <https://doi.org/10.1007/S00542-017-3342-8>.
- [81] Y. Yu, Z. Zhang, T. Zhang, X. Zhao, Y. Chen, C. Cao, Y. Li, K. Xu, Effects of surface roughness on terahertz transmission spectra, *Opt. Quantum Electron.* 52 (2020), <https://doi.org/10.1007/S11082-020-02365-X>.
- [82] P. Xie, K. Guan, D. He, H. Yi, J. Dou, Z. Zhong, Terahertz wave propagation characteristics on rough surfaces based on full-wave simulations, *Radio Sci.* 57 (2022), <https://doi.org/10.1029/2021RS007385>, e2021RS007385.
- [83] H. Wang, C.F. Pan, C. Li, K.S. Menghrajani, M.A. Schmidt, A. Li, F. Fan, Y. Zhou, W. Zhang, H. Wang, P.N.S. Nair, J.Y.E. Chan, T. Mori, Y. Hu, G. Hu, S.A. Maier, H. Ren, H. Duan, J.K.W. Yang, Two-photon polymerization lithography for imaging optics, *Int. J. Extrem. Manuf.* 6 (2024) 042002, <https://doi.org/10.1088/2631-7990/AD35FE>.
- [84] A. Siemion, The magic of optics—an overview of recent advanced terahertz diffractive optical elements, *Sensors* 21 (2020) 100, <https://doi.org/10.3390/s21010100>.
- [85] A.P. Golhin, R. Tonello, J.R. Frisvad, S. Grammatikos, A. Strandlie, Surface roughness of as-printed polymers: a comprehensive review, *Int. J. Adv. Manuf. Technol.* 3 (127) (2023) 987–1043, <https://doi.org/10.1007/S00170-023-11566-Z>, 2023 127.
- [86] R. Mendricky, D. Fris, Analysis of the accuracy and the surface roughness of FDM/FFF technology and optimisation of process parameters, *Teh. Vjesn.* 27 (2020) 1166–1173, <https://doi.org/10.17559/TV-20190320142210>.
- [87] A.S. de León, A. Domínguez-Calvo, S.I. Molina, Materials with enhanced adhesive properties based on acrylonitrile-butadiene-styrene (ABS)/thermoplastic polyurethane (TPU) blends for fused filament fabrication (FFF), *Mater. Des.* 182 (2019) 108044, <https://doi.org/10.1016/J.MATDES.2019.108044>.
- [88] M. Launhardt, A. Wörz, A. Loderer, T. Laumer, D. Drummer, T. Hausotte, M. Schmidt, Detecting surface roughness on SLS parts with various measuring techniques, *Polym. Test.* 53 (2016) 217–226, <https://doi.org/10.1016/J.POLYMERTESTING.2016.05.022>.
- [89] J. Kechagias, V. Iakovakis, E. Giorgo, P. Stavropoulos, A. Koutsomichalis, N. Vaxevanidis, Surface roughness optimization of prototypes produced by polyjet direct 3D printing technology, in: *Proceedings of the OPTI 2014 1st International Conference on Engineering and Applied Sciences Optimization*, 2014.
- [90] R. Chand, V.S. Sharma, R. Trehan, M.K. Gupta, M. Sarikaya, Investigating the dimensional accuracy and surface roughness for 3D printed parts using a multi-jet printer, *J. Mater. Eng. Perform.* 32 (2023) 1145–1159, <https://doi.org/10.1007/S11665-022-07153-0/TABLES/15>.
- [91] C. Arnold, D. Monsees, J. Hey, R. Schweyen, Surface quality of 3D-printed models as a function of various printing parameters, *Materials* 12 (2019) 1970, <https://doi.org/10.3390/MA12121970>, 2019, Vol. 12, Page 1970.
- [92] O. Bouzaglou, O. Golan, N. Lachman, Process design and parameters interaction in material extrusion 3D printing: a review, *Polymers* 15 (2023) 2280, <https://doi.org/10.3390/POLYM15102280>, 2023, Vol. 15, Page 2280.
- [93] O. Gülcen, K. Günaydin, A. Tamer, The state of the art of material jetting—a critical review, *Polymers* 13 (2021), <https://doi.org/10.3390/POLYM13162829> (Basel).
- [94] A. Mukhangaliyeva, D. Dairabayeva, A. Perveen, D. Talamona, Optimization of dimensional accuracy and surface roughness of SLA patterns and SLA-based IC components, *Polymers* 15 (2023) 4038, <https://doi.org/10.3390/POLYM15204038>, 2023, Vol. 15, Page 4038.
- [95] M. Abas, M. Al Awadh, T. Habib, S. Noor, Analyzing surface roughness variations in material extrusion additive manufacturing of nylon carbon Fiber composites, *Polymers* 15 (2023) 3633, <https://doi.org/10.3390/POLYM15173633>, 2023, Vol. 15, Page 3633.
- [96] S. Jiang, K. Hu, Y. Zhan, C. Zhao, X. Li, Theoretical and experimental investigation on the 3D surface roughness of material extrusion additive manufacturing products, *Polymers* 14 (2022) 293, <https://doi.org/10.3390/POLYM14020293>, 2022, Vol. 14, Page 293.
- [97] D. Strylbyayev, A. Seisekulova, D. Talamona, A. Perveen, The post-processing of additive manufactured polymeric and metallic parts, *J. Manuf. Mater. Process.* 6 (2022) 116, <https://doi.org/10.3390/JMMP6050116>, 2022, Vol. 6, Page 116.

- [98] G. Keane, A.V. Healy, D.M. Devine, Post-process considerations for photopolymer 3D-printed injection moulded insert tooling applications, *J. Compos. Sci.* 8 (2024) 151, <https://doi.org/10.3390/JCS8040151>, 2024, Vol. 8, Page 151.
- [99] A. Yadav, B. Poonra Prakash, K. Sai Dileep, S. Arjuna Rao, G.B. Veeresh Kumar, An experimental examination on surface finish of FDM 3D printed parts, *Mater. Today Proc.* (2023), <https://doi.org/10.1016/J.MATPR.2023.07.088>.
- [100] P. Turek, A. Bazan, A. Zakrecki, Influence of post-processing treatment on the surface roughness of polyamide PA12 samples manufactured using additive methods in the context of the production of orthoses, (2023). [10.1177/09544054231202423](https://doi.org/10.1177/09544054231202423).
- [101] A. Kantaros, T. Ganetsos, F.I.T. Petrescu, L.M. Ungureanu, I.S. Munteanu, Post-production finishing processes utilized in 3D printing technologies, *Processes* 12 (2024) 595, <https://doi.org/10.3390/PR12030595>, 2024, Vol. 12, Page 595.
- [102] J.V. Chen, A.B.C. Dang, A. Dang, Comparing cost and print time estimates for six commercially-available 3D printers obtained through slicing software for clinically relevant anatomical models, *3D Print. Med.* 7 (2021) 1, <https://doi.org/10.1186/s41205-020-00091-4>.
- [103] M. Kutz, *Applied Plastics Engineering Handbook : Processing, Materials, and Applications*, 2nd ed., Elsevier, 2016.
- [104] 3DA solutions, selective laser melting, 3DA Solutions (2019).
- [105] J. Go, S.N. Schiffres, A.G. Stevens, A.J. Hart, Rate limits of additive manufacturing by fused filament fabrication and guidelines for high-throughput system design, *Addit. Manuf.* 16 (2017) 1–11, <https://doi.org/10.1016/J.ADDMA.2017.03.007>.
- [106] 3D Systems, ProJet MJP 2500W Plus, (2023).
- [107] M. Kaluza, M. Walczakowski, A. Siemion, Exploring the impact of 3D printing parameters on the THz optical characteristics of COC material, *Materials* 17 (2024) 5104, <https://doi.org/10.3390/MA17205104>, 2024, Vol. 17, Page 5104.
- [108] M. Mao, J. He, X. Li, B. Zhang, Q. Lei, Y. Liu, D. Li, The emerging frontiers and applications of high-resolution 3D printing, *Micromachines* 8 (2017) 113, <https://doi.org/10.3390/M8040113>, 2017, Vol. 8, Page 113.
- [109] N.A. Sukindar, M.K.A. Ariffin, B.T. Hang Tuah Baharudin, C.N.A. Jaafar, M.I. S. Ismail, Analyzing the effect of nozzle diameter in fused deposition modeling for extruding polylactic acid using open source 3D printing, *J. Teknol.* 78 (2016) 7–15, <https://doi.org/10.11113/JT.V78.6265>.
- [110] P. Czyzewski, D. Marciniak, B. Nowinka, M. Borowiak, M. Bieliński, Influence of extruder's nozzle diameter on the improvement of functional properties of 3D-printed PLA products, *Polymers* 14 (2022) 356, <https://doi.org/10.3390/polym14020356> (Basel).
- [111] R.F. Quero, G. Domingos Da Silveira, J.A. Fracassi Da Silva, D.P. De Jesus, Understanding and improving FDM 3D printing to fabricate high-resolution and optically transparent microfluidic devices, *Lab Chip* 21 (2021) 3715–3729, <https://doi.org/10.1039/D1LC00518A>.
- [112] N.C. Zuchowicz, J.A. Belgodere, Y. Liu, I. Semmes, W.T. Monroe, T.R. Tiersch, Low-cost resin 3-D printing for rapid prototyping of microdevices: opportunities for supporting aquatic germplasm repositories, *Fishes* 49 (7) (2022) 49, <https://doi.org/10.3390/FISHES7010049>, 2022, Vol. 7, Page.
- [113] M.C. Sow, T. De Terris, O. Castelnaud, Z. Hamouche, F. Coste, R. Fabbro, P. Peyre, Influence of beam diameter on Laser Powder Bed Fusion (L-PBF) process, *Addit. Manuf.* 36 (2020), <https://doi.org/10.1016/J.ADDMA.2020.101532>.
- [114] S.C. Ligon, R. Liska, J. Stampfl, M. Gurr, R. Mülhaupt, Polymers for 3D printing and customized additive manufacturing, *Chem. Rev.* 117 (2017) 10212–10290, <https://doi.org/10.1021/acs.chemrev.7b00074>.
- [115] A. Shannon, A. O'Connell, A. O'Sullivan, M. Byrne, S. Clifford, K.J. O'Sullivan, L. O'Sullivan, A radiopaque nanoparticle-based ink using PolyJet 3D printing for medical applications, *3D Print. Addit. Manuf.* 7 (2020) 259, <https://doi.org/10.1089/3DP.2019.0160>.
- [116] M. Pagac, J. Hajnys, Q.P. Ma, L. Jancar, J. Jansa, P. Stefek, J. Mesicek, A review of Vat photopolymerization technology: materials, applications, challenges, and future trends of 3D printing, *Polymers* 13 (2021) 598, <https://doi.org/10.3390/polym13040598> (Basel).
- [117] J.L. Saorin, M.D. Diaz-Alemán, J. De la Torre-Cantero, C. Meier, I. Pérez Conesa, Design and validation of an open source 3D printer based on digital ultraviolet light processing (DLP), for the improvement of traditional artistic casting techniques for microsculptures, *Appl. Sci.* 11 (2021) 3197, <https://doi.org/10.3390/app11073197>.
- [118] W.J. Otter, N.M. Ridler, H. Yasukochi, K. Soeda, K. Konishi, J. Yumoto, M. Kuwata-Gonokami, S. Lucyszyn, Printing: the future of THz, *Electron. Lett.* 53 (2017) 443, <https://doi.org/10.1049/el.2017.0943>.
- [119] X. Guo, Z. Xue, Y. Zhang, Manufacturing of 3D multifunctional microelectronic devices: challenges and opportunities, *NPG Asia Mater.* 11 (2019) 1–7, <https://doi.org/10.1038/s41427-019-0129-7>, 2019 11:1.
- [120] D. Behera, S. Chizari, L.A. Shaw, M. Porter, R. Hensleigh, Z. Xu, X. Zheng, L. G. Connolly, N.K. Roy, R.M. Panas, S.K. Saha, X. (Rayne) Zheng, J.B. Hopkins, S. C. Chen, M.A. Cullinan, Current challenges and potential directions towards precision microscale additive manufacturing—part IV: future perspectives, *Precis. Eng.* 68 (2021) 197–205, <https://doi.org/10.1016/J.PRECISIONENG.2020.12.014>.
- [121] Y.G. Park, I. Yun, W.G. Chung, W. Park, D.H. Lee, J.U. Park, High-resolution 3D printing for electronics, *Adv. Sci.* 9 (2022) 2104623, <https://doi.org/10.1002/ADVS.202104623>.
- [122] M.A.S.R. Saadi, A. Maguire, N.T. Pottackal, M.S.H. Thakur, M.Md. Ikram, A. J. Hart, P.M. Ajayan, M.M. Rahman, Direct ink writing: a 3D printing technology for diverse materials, *Adv. Mater.* 34 (2022) 2108855, <https://doi.org/10.1002/adma.202108855>.
- [123] Y. Li, B. Li, Direct ink writing 3D printing of polydimethylsiloxane-based soft and composite materials: a mini review, *Oxf. Open Mater. Sci.* 2 (2022), <https://doi.org/10.1093/OXFMAT/ITAC008>.
- [124] S. Ramesh, C. Mahajan, S. Gerdes, A. Gaikwad, P. Rao, D.R. Cormier, I.V. Rivero, Numerical and experimental investigation of aerosol jet printing, *Addit. Manuf.* 59 (2022), <https://doi.org/10.1016/J.ADDMA.2022.103090>.
- [125] J. Park, M. Hardy, S. Jun Kang, K. Barton, K. Adair, D. Kishore Mukhopadhyay, C. Young Lee, M.S. Strano, A.G. Alleyne, J.G. Georgiadis, P.M. Ferreira, J.A. Rogers, High-resolution electrohydrodynamic jet printing efforts to adapt and extend graphic arts printing techniques for demanding device applications in electronics, biotechnology and microelectromechanical systems have grown rapidly in recent years, (2007). [10.1038/nmat1974](https://doi.org/10.1038/nmat1974).
- [126] B. Zhang, B. Seong, V. Nguyen, D. Byun, 3D printing of high-resolution PLA-based structures by hybrid electrohydrodynamic and fused deposition modeling techniques, *J. Micromech. Microeng.* 26 (2016) 025015, <https://doi.org/10.1088/0960-1317/26/2/025015>.
- [127] M. Al-Abaddi, L. Sasso, M. Dimaki, W.E. Svendsen, Fabrication of 3D nano/microelectrodes via two-photon-polymerization, (2012). [10.1016/j.mee.2012.07.015](https://doi.org/10.1016/j.mee.2012.07.015).
- [128] F. Zhang, L. Zhu, Z. Li, S. Wang, J. Shi, W. Tang, N. Li, J. Yang, The recent development of vat photopolymerization: a review, *Addit. Manuf.* 48 (2021) 102423, <https://doi.org/10.1016/J.ADDMA.2021.102423>.
- [129] A. Ottomaniello, P. Vezio, O. Trincinci, F.M. Den Hoed, P. Dean, A. Tredicucci, V. Mattoli, Highly conformable terahertz metasurface absorbers via two-photon polymerization on polymeric ultra-thin films, *Nanophotonics* 12 (2023) 1557–1570, <https://doi.org/10.1515/NANOPH-2022-0667>.
- [130] J.F. Xing, X.Z. Dong, W.Q. Chen, X.M. Duan, N. Takeyasu, T. Tanaka, S. Kawata, Improving spatial resolution of two-photon microfabrication by using photoinitiator with high initiating efficiency, *Appl. Phys. Lett.* 90 (2007) 131106, <https://doi.org/10.1063/1.2717532>.
- [131] E.B. Secor, Principles of aerosol jet printing, *Flex. Print. Electron.* 3 (2018) 035002, <https://doi.org/10.1088/2058-8585/AACE28>.
- [132] X. Kong, H. Li, J. Wang, Y. Wang, L. Zhang, M. Gong, X. Lin, D. Wang, Direct writing of silver nanowire patterns with line width down to 50 µm and ultrahigh conductivity, *ACS Appl. Mater. Interfaces* (2023), <https://doi.org/10.1021/acsaami.2c22885>.
- [133] K. Muldoon, Y. Song, Z. Ahmad, X. Chen, M.W. Chang, High precision 3D printing for micro to nano scale biomedical and electronic devices, *Micromachines* 13 (2022), <https://doi.org/10.3390/mi13040642> (Basel).
- [134] C. Oakley, P. Chahal, Aerosol jet printed quasi-optical terahertz components, *IEEE Trans. Terahertz Sci. Technol.* 8 (2018) 765–772, <https://doi.org/10.1109/TTHZ.2018.2873915>.
- [135] A. Zhakeyev, P. Wang, L. Zhang, W. Shu, H. Wang, J. Xuan, Additive manufacturing: unlocking the evolution of energy materials, *Adv. Sci.* 4 (2017) 1700187, <https://doi.org/10.1002/ADVS.201700187>.
- [136] J. Kennedy, L. Flanagan, L. Dowling, G.J. Bennett, H. Rice, D. Trimble, The influence of additive manufacturing processes on the performance of a periodic acoustic metamaterial, *Int. J. Polym. Sci.* 2019 (2019), <https://doi.org/10.1155/2019/7029143>.
- [137] M.J. Beauchamp, G.P. Nordin, A.T. Woolley, Moving from millifluidic to truly microfluidic sub-100-µm cross-section 3D printed devices, *Anal. Bioanal. Chem.* 409 (2017) 4311–4319, <https://doi.org/10.1007/S00216-017-0398-3>.
- [138] A. Rogers, Prototyping with POLYJET 3D PRINTING, *Appl. Des.* 65 (2017) 25–26. <https://go.openathens.net/redirector/leeds.ac.uk?url=https://www.proquest.com/trade-journals/prototyping-with-polyjet-3d-printing/docview/2103551139/se-2?accountid=14664>.
- [139] C. Gu, F. Cheng, S. Gao, D-band antenna-filter integration using metal 3D printing, in: Proceedings of the UCMMT 2021–UK–Europe–China Workshop on Millimetre-Waves and Terahertz Technologies, 2021, <https://doi.org/10.1109/UCMMT53364.2021.9569862>.
- [140] Z. Huang, G. Shao, L. Li, Micro/nano functional devices fabricated by additive manufacturing, *Prog. Mater. Sci.* 131 (2023) 101020, <https://doi.org/10.1016/J.PMATSCI.2022.101020>.
- [141] R.A. Bahr, A.O. Adeyeye, S. Van Rijs, M.M. Tentzeris, 3D-Printed omnidirectional Luneburg lens retroreflectors for low-cost mm-wave positioning, in: Proceedings of the IEEE International Conference on RFID, RFID 2020, 2020, <https://doi.org/10.1109/RFID49298.2020.9244891>.
- [142] Z. Xu, Y. Wang, D. Wu, K.P. Ananth, J. Bai, The process and performance comparison of polyamide 12 manufactured by multi jet fusion and selective laser sintering, *J. Manuf. Process.* 47 (2019) 419–426, <https://doi.org/10.1016/J.JMAPRO.2019.07.014>.
- [143] S. Barone, P. Neri, A. Paoletti, A.V. Razonale, F. Tamburrino, Development of a DLP 3D printer for orthodontic applications, *Procedia Manuf.* 38 (2019) 1017–1025, <https://doi.org/10.1016/J.PROMFG.2020.01.187>.
- [144] L. Love, B. Post, M. Noakes, A. Nycz, V. Kunc, There's plenty of room at the top, *Addit. Manuf.* 39 (2020), <https://doi.org/10.1016/J.ADDMA.2020.101727>.
- [145] F. Pignatelli, G. Percoco, An application- and market-oriented review on large format additive manufacturing, focusing on polymer pellet-based 3D printing, *Prog. Addit. Manuf.* 7 (2022) 1363–1377, <https://doi.org/10.1007/S40964-022-00309-3>.
- [146] M. Wiese, A. Kwauka, S. Thiede, C. Herrmann, Economic assessment for additive manufacturing of automotive end-use parts through digital light processing (DLP), *CIRP J. Manuf. Sci. Technol.* 35 (2021) 268–280, <https://doi.org/10.1016/J.CIRPJ.2021.06.020>.

- [147] X. Li, W. Lu, X. Xu, Y. Wang, S.C. Chen, Advanced optical methods and materials for fabricating 3D tissue scaffolds, *Light Adv. Manuf.* 3 (2022) 493–524, <https://doi.org/10.37188/LAM.2022.026>.
- [148] X. Shi, S. Ma, C. Liu, C. Chen, Q. Wu, X. Chen, J. Lu, Performance of high layer thickness in selective laser melting of Ti6Al4V, *Materials* 9 (2016), <https://doi.org/10.3390/MA9120975>.
- [149] CDG, ProJet 2500W plus MJP wax, (2023).
- [150] C. Schwaar, All the new professional 3D printers launched in 2023, All3DP (2023).
- [151] X. Zhou, Y. Hou, J. Lin, A review on the processing accuracy of two-photon polymerization, *AIP Adv.* 5 (2015) 030701, <https://doi.org/10.1063/1.4916886>.